Effects of Phloretin on Three Types of Chloride Channels in Epithelial Cells

Hai-Tian Fan

Department of Physiological Sciences
School of Life Science
Graduate University for Advanced Studies
and
Department of Cell Physiology
National Institute for Physiological Sciences
Okazaki, 444-8585, Japan
1999

ABSTRACT

Phloretin, which is the aglucon of phloridzin, has been widely used as an inhibitor of glucose transporter. Since we have recently found that phloretin inhibits a regulatory volume decrease after osmotic swelling in a human epithelial cell line, in the present study, I investigated the effects of phloretin on volume-sensitive Cl^- channels using three different epithelial cell lines by the whole-cell patch-clamp technique. Extracellular application of phloretin (over 10 μM) was found to inhibit, in a concentration-dependent manner (IC_{50} ~ 20 μM), the volume-sensitive Cl^- current activated by a hypotonic challenge in human epithelial T84 and Intestine 407 cells as well as in mouse epithelial C127/CFTR cells. In contrast, at a low concentration (30 μM), phloretin failed to inhibit CFTR Cl^- currents activated by cAMP stimulation in T84 and C127/CFTR cells. At a high concentration (300 μM), however, partial inhibition by phloretin was observed in the CFTR Cl^- currents in both cell types. At 30 and 300 μM, on the other hand, phloretin showed no inhibitory effect on Ca^{2+}-activated Cl^- currents induced by ionomycin in human T84 cells but rather reactivated them after inactivation during stimulation with ionomycin. It is concluded that phloretin is a novel inhibitor of volume-sensitive Cl^- channel, and that at low concentrations phloretin specifically blocks this channel without inhibiting both cAMP-activated and Ca^{2+}-activated Cl^- channels in epithelial cells.

INTRODUCTION

Cell volume regulation is of fundamental importance in mammalian cells under anisotonic conditions, for keeping cell structural integrity and a variety of cellular functions (Okada, 1998; Lang, 1998). In response to a hypotonic external solution, cells swell and then gradually recover their original volume. This process, known as a regulatory volume decrease (RVD), involves the effluxes of KCl as well as organic solutes including some amino acids (for reviews see Okada, 1997; Strange et al., 1996). As intracellular solutes are lost, water follows passively according to the osmotic gradient across cell membranes. Different pathways have been proposed for the efflux of KCl in different types of cells (see Okada, 1997). As those for anions, three types of chloride channels have lately attracted considerable attention. A volume-sensitive Cl^- channel, which is thought to be the most important anion channel for RVD in many cell types, has been extensively studied, and its electrophysiological characteristics, such as outward rectification and voltage-dependent inactivation, are well described since ten years ago (see Okada, 1997). However, its molecular identity and activation mechanism are still unclear (Okada, 1997; Okada et al., 1998), though a ClC-3 gene of the ClC family of voltage-gated Cl^- channels was reported to encode a volume-sensitive Cl^- channel (Duan et al., 1997). The cloning of the gene encoding this Cl^- channel has been quite difficult, because most cell types express endogenously this channel thereby preventing the expression cloning, and because overexpression of candidate genes or proteins often upregulates the activity of endogenous

anion channels (see Okada, 1997). Thus, it would be greatly helpful for the cloning if a highly specific blocker, which is useful for the protein purification, of this channel were discovered.

In epithelial cells, there exist two other major types of anion channels, cAMP-activated and Ca^{2+}-activated Cl^- channels, in addition to volume-sensitive Cl^- channels. The phenotypical characteristics of these three types are summarized in Table 1. CFTR (cystic fibrosis transmembrane conductance regulator) was found as the product of the cystic fibrosis gene at first. It is now known as a multifunctional protein, a member of the ATP-binding cassette (ABC) superfamily of membrane proteins, that functions not only as a cAMP-activated epithelial Cl^- channel but also as a regulator of other channels and transporters (see Kunzelmann & Schreiber, 1999; Schwiebert et al., 1999). This channel can be activated by phosphorylation of its regulatory domain. In cardiac myocytes, activation of CFTR under stimulation of ß-adrenergic receptors was reported to be responsible for Cl^- efflux during the RVD (Wang et al., 1997). However, under physiological conditions, it is not precisely determined which is a main anion pathway, CFTR or volume-sensitive Cl^- channel for RVD in CFTR-expressing cells. In many cell types, an increase in intracellular free Ca^{2+} has been observed under hypotonic conditions (see McCarty & O'Neil, 1992; Okada, 1997). It is well known that strongly outwardly rectifying Cl^- currents can be activated by elevation of intracellular Ca^{2+} concentration in many cell types (Findlary & Petersen, 1985; Evans & Marty, 1986; Welsh, 1986; Taleb et al., 1988; Cliff & Frizzell, 1990; Krause & Welsh, 1990; Zygmunt & Gibbons, 1991; Kunzelmann et al., 1992; Pedersen et al., 1998). Little is

known about an involvement of Ca^{2+}-activated Cl^- channel in RVD so far. In Cl^- secreting epithelial cells both CFTR and Ca^{2+}-activated Cl^- channels are known to be operating in concert for Cl^- and fluid secretion. It is also known that a Ca^{2+}-activated secretory pathway for Cl^- may act as a substitute for CFTR in various tissues of cystic fibrosis patients and CFTR knockout mice (Wagner et al., 1992; Rozmahel et al., 1996). However, it is not known whether volume-sensitive Cl^- channels are, if any, involved in epithelial anion secretion under physiological or pathological conditions. Therefore, it would be very useful if a highly specific blocker for each channel were available to discriminate functionally from each other. However, no specific blocker is known for volume-sensitive Cl^- channels, as summarized in Table 1.

Phloretin is the aglucon of phlorizin (Table 2), a sap-soluble pigment extracted from the root bark of apple trees (Seshadri, 1951), which is known to inhibit Na^+-independent glucose transmembrance transport (Sahagian, 1965; Betz et al., 1975; Kasahara & Kasahara, 1996) as well as protein kinase C (PKC) (Gschwendt et al., 1984) and to cause apoptosis in B16 mouse melanoma cells (Kobori et al., 1997). Moreover, it has recently been reported that this compound is an inhibitor of aquaporin-3 water channel and urea transporter (Ishibashi et al., 1994; Echevarria et al., 1996). As to cation channels, phloretin was also found to block L-type Ca^{2+} channels in pituitary adenoma cells (Prevarskaya et al., 1994) but enhance endogenous Ca^{2+}-activated K^+ channels in amphibian myelinated nerve fibers (Koh et al., 1994) and the cloned *Slo* channels (Gribkoff et al., 1996). Activation of Ca^{2+}-dependent K^+ channels is known to be one of the causal

factors leading to RVD in many epithelial cells (see Okada, 1997), as originally demonstrated in Intestine 407 cells (Hazama & Okada, 1988). Our recent study (Fan et al., 2000) by a high-speed automatic image analyzing technique (Morishima et al., 1998), however, showed that phloretin (300 μM) completely inhibited the RVD of Intestine 407 cells under hypotonic conditions (Fig. 1). Thus, there is a possibility that phloretin inhibits the RVD in Intestine 407 cells by impairing the Cl^- pathway. Phloretin was shown to have no effect on the Ca^{2+}-activated Cl^- conductance in T84 cells at 50 μM (Worrell & Frizzell, 1991) and on the cAMP-activated Cl^- current in CFTR-expressing *Xenopus* oocytes at 350 μM (Schreiber et al., 1997). However, whether phloretin specifically inhibits the volume-sensitive Cl^- channel is still a riddle.

In the present study, thus, I investigated the effects of phloretin on volume-sensitive Cl^- channels as well as cAMP-activated and Ca^{2+}-activated Cl^- channels in human colonic T84 cells which are known to express these three types of Cl^- channels (Worrell et al., 1989; Cliff & Frizzell, 1990; Chang et al., 1992; Merlin et al., 1998), using the whole-cell patch-clamp technique. Since there may be a possibility that phloretin exhibits different effects on these channels in different cell types, I employed two other epithelial cell lines: human Intestine 407 cells, in which properties of volume-sensitive Cl^- channels were most extensively studied (Kubo & Okada, 1992; Tominaga et al., 1995; Tsumura et al., 1996; Liu et al., 1998; Hazama et al., 1999) and mouse mammary C127 cells stably transfected with cDNA for CFTR (C127/CFTR cells), which express not only cAMP-activated Cl^- channels but also volume-sensitive Cl^-

channels (Hazama et al., 2000).

MATERIALS AND METHODS

Cell culture

T84 cells were obtained from the American Type Culture Collection (ATCC No. CCL-248, Rockville, MD., USA) and grown at 37°C in a 25 cm^2 flask gassed with 95% O_2 and 5% CO_2. The monolayers were cultured in ATCC medium composed of a 95% 1:1 mixture of Ham's F12 medium and Dulbecco's modified Eagle's medium supplemented with 2.5 mM L-glutamine and 5% fetal bovine serum, as reported previously (Arreola et al., 1995). For patch clamp studies, cells were dispersed by incubating them for 20 min with Ca^{2+}- and Mg^{2+}-free Dulbecco's phosphate buffered saline (Ca^{2+}-, Mg^{2+}-free PBS). Cells on 10 mm diameter glasscover slips (Matsunami Glass Ind., LTD) were studied 1-3 days after planting.

A human intestinal epithelial cell line, Intestine 407, was cultured in monolayer in Fischer medium supplemented with 10% newborn calf serum under a 95% O_2-5% CO_2 atmosphere, as described previously (Kubo & Okada, 1992). Before patch-clamp experiments, the monolayer of cells was isolated to single spherical cells by pipetting, and was cultured in suspension with agitation for 15–240 min.

A stable transfectant of C127i, which is a mouse mammary adenocarcinoma cell line, with the cDNA for human CFTR (C127/CFTR) was a kind gift of Dr. M. J. Welsh (University of Iowa). C127/CFTR cells were cultured in monolayer in Dulbecco's modified Eagle's medium (DMEM, High Glucose) with 10% fetal bovine serum (FBS) and 200 μg/ml geneticin. Single cells were prepared by washing the monolayer with

Ca^{2+}- and Mg^{2+}-free Hanks' balanced salt solution (Ca^{2+}-, Mg^{2+}-free HBSS) twice then incubating with 0.25% trypsin-EDTA/PBS solution, and cultured in suspension with agitation for 10–180 min before using in patch-clamp experiments.

Patch-clamp whole-cell recordings

Whole-cell recordings were performed with wide-tipped electrodes (around 2 MΩ) fabricated from haematocrit capillaries by Brown-Flaming Micropipette Puller (Model P-97, Sutter Instrument Co., USA), as reported previously (Kubo & Okada, 1992; Liu et al., 1998; Hazama et al., 2000). Series resistance (<5 MΩ) was compensated (about 75%) to minimize voltage errors in experiments on volume-sensitive Cl^- currents. The time course of current activation and recovery was monitored by repetitively applying (every 15 s) alternating step pulses (2-s duration) from a holding potential of 0 mV to ±40 (or ±80) mV for volume-sensitive and Ca^{2+}-activated Cl^- currents, and ramp pulses from a holding potential of 0 mV to ±100 (or ±80) mV for cAMP-activated Cl^- currents in C127/CFTR cells. As to cAMP-activated Cl^- currents in T84 cells, the membrane potential was held at –20 mV and alternating step pulses to 0 mV and –84 mV were repetitively applied to monitor the time course of current activation and recovery. To monitor the time and voltage dependence of volume-sensitive Cl^- currents, the membrane potential was held at –80 mV and step pulses (2-s duration) were applied from a pre-potential at –100 mV (0.2-s duration) to test potentials of –100 to +100 (or +80) mV in 20-mV increments. For recordings of cAMP-activated and Ca^{2+}-activated Cl^-

currents, the membrane potential was held at 0 mV and step pulses (1-s duration) from −100 to +100 mV in 20-mV increments were applied.

Currents were recorded using an Axopatch 200A amplifier (Axon Instruments, Foster City, CA). Current signals were filtered at 1 kHz using a 4-pole Bessel-filter and digitized at 4 kHz. The pCLAMP software (version 6.0.2; Axon Instruments) was used for command control, data acquisition and analysis.

Bath solution was maintained at 37°C in experiments on cAMP-activated Cl^- currents in T84 cells. All other experiments were carried out at room temperature (23–26°C). Data are given as means ± SE. Statistical differences of the data were evaluated by Student's *t*-test and were considered significant at $P < 0.05$.

Solution and chemicals

For experiments on volume-sensitive Cl^- currents, isotonic bath solution (osmolality 330 mosmol/kgH_2O) contained (in mM) 110 CsCl, 5 $MgSO_4$, 100 mannitol, 12 HEPES, and 8 tris(hydroxymethy)amino-methane (Tris), adjusted to pH 7.4 with H_2SO_4. Hypotonic bath solution (osmolality 270 mosmol/kgH_2O) was prepared by reducing mannitol to 40 mM. In some experiments, the CsCl concentration was reduced to 11 mM by replacing with mannitol. Pipette solution (osmolality 300 mosmol/kgH_2O) contained (in mM) 110 CsCl, 2 $MgSO_4$, 1 EGTA, 1 Na_2-ATP, 50 mannitol, and 15 Na-HEPES, adjusted to pH 7.4 with H_2SO_4. For the experiments on cAMP-activated Cl^- currents in C127/CFTR cells, osmolality of isotonic bath solution was maintained at 310 mosmol/kgH_2O by reducing mannitol to 80

mM, and the concentrations of Na_2-ATP and mannitol in the pipette solution were changed to 2 mM and 47 mM, respectively.

The solutions employed in experiments on cAMP-activated Cl^- currents with T84 cells were as those described previously (Cliff & Frizzell, 1990). Bath solution contained (in mM): 115 NaCl, 40 *N*-methyl-D-glucamine (NMDG) glutamate, 5 potassium glutamate, 2 $MgCl_2$, 1 $CaCl_2$, and 5 HEPES, adjusted to pH 7.3 with NaOH (osmolality 330 mosmol/kgH_2O). Pipette solution (osmolality 300 mosmol/kgH_2O) contained (in mM): 115 KCl, 25 NMDG glutamate, 0.5 EGTA, 0.19 $CaCl_2$, 2 $MgCl_2$, 2 Na_2ATP, 0.05 Na_3GTP, and 5 HEPES, adjusted to pH 7.3 with KOH. Na^+- and K^+-free solution containing $NMDG^+$ was used in the experiments on Ca^{2+}-activated Cl^- currents in T84 cells. In some experiments, Na^+ and K^+ were replaced with $NMDG^+$, and a part of Cl^- was replaced with glutamate to change the equilibrium potential to Cl^-.

The composition of Ca^{2+}-, Mg^{2+}-free HBSS was (in mM): 5.36 KCl, 0.441 KH_2PO_4, 136.7 NaCl, 4.17 $NaHCO_3$, 0.385 Na_2HPO_4, 5.55 D-glucose (pH 7.3).

Trypsin-EDTA/PBS solution was (in mM): 113 Na_2HPO_4, 1.69 KH_2PO_4, 0.2% EDTA, 0.25% trypsin (pH 7.3).

Forskolin, N^6, O^7-dibutyryl adenosine 3', 5'-cyclic monophosphate sodium salt (dbcAMP) and calphostin C were obtained from Wako Chemicals (Osaka, Japan), and other chemicals were from Sigma (St. Louis, MO). Stock solutions of phloretin, calphostin C and 3-isobutyl-1-methylxanthine (IBMX) in dimethyl sulfoxide (DMSO), and those of forskolin, ionomycin and phloridzin in ethanol were diluted to the desired

final concentrations just before use. DMSO or ethanol concentration never exceeded 0.1% and had no effect on whole-cell currents.

RESULTS

Effects of phloretin and phloridzin on volume-sensitive Cl^- currents

Whole-cell currents recorded in T84 cells under isotonic bath solution were trifling. Upon exposure to 82% hypotonic bath solution, activation of outwardly rectifying currents (Fig. 2A), that exhibited time-dependent inactivation at large positive potentials (Fig. 2B), was observed in T84 cells. As shown in Fig. 3, the reversal potential was shifted by about +40 mV (41.4 ± 3.6 mV, n=4), when the bath Cl^- concentration was reduced from 110 mM to 11 mM. Thus, activated currents are considered to be volume-sensitive Cl^- currents, as reported previously (Worrell et al., 1989). Extracellular application of phloretin at the concentration of 30 μM significantly suppressed the currents, and 300 μM phloretin almost completely inhibited the volume-sensitive Cl^- currents (Fig. 2) in the entire voltage range examined (Fig. 4). The effect of phloretin was rapid in onset and reversible (Fig. 2). There was no obvious voltage dependence of the inhibitory effect of phloretin, as the inward and outward currents were inhibited to the essentially same degree (Fig. 5).

The time course of inactivation observed upon large depolarization could be fitted by a double exponential function (Fig. 6A), as was the case of Intestine 407 cells (Tsumura et al., 1996; Liu et al., 1998). Both the fast (τ_f) and slow time constants (τ_s) were not significantly affected by 30 μM phloretin (Fig. 6B).

The inhibitory effect of phloretin was further investigated in Intestine

407 cells, which do not possess CFTR mRNA (Hazama et al., 1998) and Ca^{2+}-activated Cl^- currents (Tilly et al., 1994). As observed in T84 cells, extracellular phloretin suppressed the volume-sensitive Cl^- current in Intestine 407 cells in a concentration-dependent manner (Fig. 7). The concentration for half-maximal inhibition (IC_{50}) was estimated to be 20.4 ± 5.9 μM by a sigmoidal fitting (Fig. 8). The inhibiting effect in Intestine 407 cells was also a voltage-independence (data not shown, n=10), as that observed in T84 cells. On the contrary, when incorporated in the pipette (intracellular) solution, phloretin failed to inhibit the volume-sensitive Cl^- current even at a high concentration (300 μM) (Fig. 9).

Similar anion currents could also be activated by hypotonic stress in C127 mouse mammary epithelial cells stably transfected with CFTR (C127/CFTR cells) under hypotonic conditions (Fig. 10A). Reduction of bath Cl^- from 110 mM to 11 mM by replacement with mannitol induced a shift of E_{rev} by 40.1 ± 3.2 mV (n=3), confirming that these currents were anion selective (Fig. 10B). Phloretin also inhibited the volume-sensitive Cl^- current in C127/CFTR cells (Fig. 10A) in a voltage-independent manner (Fig. 11). The inhibitory effect of phloretin on the volume-sensitive Cl^- current in C127/CFTR cells was also reversible (data not shown, n=2). Concentration dependence of the phloretin effect in C127/CFTR cells (Fig. 11) was similar to that in T84 cells (Fig. 4) and Intestine 407 cells (Fig. 8).

In contrast to phloretin, extracellular phloridzin, a glucoside of phloretin, showed no effect on the volume-sensitive Cl^- current even though at a concentration as high as 1 mM in T84 cells (data not shown, n=3) and Intestine 407 cells (Fig. 12). PKC is known to be inhibited not only by

phloretin (Gschwendt et al., 1984) but also by phloridzin (Shoji et al., 1997). Therefore, it is unlikely that the phloretin effect on volume-sensitive Cl^- currents was mediated by inhibition of PKC. Actually, calphostin C (500 nM), which is a specific inhibitor of PKC with an IC_{50} of 50 nM (Kobayashi et al., 1989), did not affect the volume-sensitive Cl^- current in Intestine 407 cells under hypotonic conditions (Fig. 13).

Effects of phloretin on Ca^{2+}-activated Cl^- currents

In T84 (but not Intestine 407 and C127/CFTR) cells whole-cell current were activated rapidly by adding a Ca^{2+} ionophore, ionomycin (1–2.5 μM), to isotonic bath solution containing 1 mM Ca^{2+} in a reversible manner (Fig. 14A). After reaching the maximum amplitude the activated current gradually run down and soon reached a plateau level (Fig. 14A). The ionomycin-induced current showed marked outward rectification and unique time-dependent behavior (Fig. 14B). The currents exhibited time-dependent activation at positive potentials and inactivation kinetics at negative potentials. The reversal potential was shifted by 31.1 ± 0.9 mM (n=5), when the bath Cl^- concentration was reduced from 121 mM to 19 mM, the fact indicating the anionic nature (Fig. 14C). When 30 μM phloretin was applied to bath solution after ionomycin-induced currents had attained the steady-state level, inhibition of the current was never observed but consistently caused a significant increase in the amplitude of the currents (Fig. 15A). The reactivated current in the presence of phloretin also exhibited similar voltage-dependent inactivation and activation kinetics (Fig. 15B) and outward rectification (Fig. 15C). Furthermore,

reduction of bath Cl^- concentration from 121 mM to 19 mM, the reversal potential shifted according to a change in the equilibrium potential to Cl^- (E_{Cl}) (data not shown, n=3). Essentially same effects on Ca^{2+}-activated Cl^- currents were observed with 300 μM phloretin (data not shown, n=2). In the absence of ionomycin, no current was activated by 30 μM phloretin added to the bath solution containing 1 mM Ca^{2+} (Fig. 16A). Prominent activation of currents was thereafter induced by ionomycin (Fig. 16A). Ionomycin-induced activation of Cl^- currents was sustained for a longer time in the presence of phloretin than that in the absence of phloretin. However, the peak amplitude of ionomycin-induced currents in the presence of 30 μM phloretin was not significantly larger than those in the absence of phloretin (Fig. 16B).

Effects of phloretin on cAMP-activated Cl^- currents

A cocktail of forskolin (10 μM), dbcAMP (500 μM) and IBMX (400 μM) induced rapidly activation of currents in a reversible manner in T84 cells (Fig. 17A). Current responses to step pulses demonstrated no time-dependent activation and inactivation (Fig. 17B). The current-voltage (I-V) curve showed a linear relationship over the voltage range between −100 mV and +100 mV, and the reversal potential was close to 0 mV, as expected for a Cl^- current (Fig. 17C). Furthermore, the reversal potential was shifted by 45.8 ± 4.4 mV (n=4), when the bath Cl^- concentration was reduced from 110 mM to 11 mM. On the other hand, the cocktail activated the current at −84 mV which was equal to the equilibrium potential to K^+ (E_K), whereas no current activation was induced at 0 mV which was equal to E_{Cl} (Fig.

17A). These results indicate that the cAMP-activated current has characteristic of the CFTR-type Cl^- current. No effect of phloretin was observed at 30 μM on the cAMP-activated current (Fig. 17). However, when the phloretin concentration was increased to 300 μM, the inward component of cAMP-activated Cl^- currents was significantly inhibited, without producing significant changes in the outward component (Fig. 18). Even at 600 μM phloretin-induced inhibition of cAMP-activated Cl^- currents was not complete and was voltage-dependent (Fig. 19). The IC_{50} of phloretin was 252.0 ± 20.7 μM for the inward component and 474.7 ± 24.5 μM for the outward component of the Cl^- current. On the contrary, such inhibitory effects were not caused by intracellular application of 300 μM phloretin (Fig. 20).

In C127/CFTR (but not Intestine 407) cells, whole-cell CFTR-type Cl^- currents could also be activated by the cocktail of forskolin (10 μM), dbcAMP (500 μM) and IBMX (400 μM), as reported previously (Hazama et al., 2000). Application of 30 μM phloretin showed no effect on both the inward and outward components of cAMP-activated Cl^- currents (Fig. 21). However, 300 μM phloretin, though in part, suppressed the cAMP-activated Cl^- currents in C127/CFTR cells (Fig. 22). The outward component was also significantly diminished by 300 μM phloretin, although this inhibition was less marked than the inhibition of the inward component. In contrast, calphostin C (500 nM) failed to affect cAMP-induced current in C127/CFTR cells (Fig. 23).

DISCUSSION

Phloretin is a well-known inhibitor of Na^+-independent glucose transporter (glucose uniporter: GLUT) (Betz et al., 1975; Krupka, 1985; Sahagian, 1965), whereas phloridzin, a glucoside of phloretin, is a specific inhibitor of Na^+-dependent glucose transporter (Na^+-glucose symporter: SGLT) (Betz et al., 1975, Loo et al., 1999; Sahagian, 1965). The present study demonstrated that phloretin, but not phloridzin, is a potent inhibitor of volume-sensitive Cl^- channels in epithelial cells. This fact can well explain our previous finding that phloretin (300 μM) inhibits the RVD of Intestine 407 cells after osmotic swelling (Fan et al., 2000). However, this fact may not exclude the possibility that phloretin inhibits other channels which are involved in the RVD mechanism. In Intestine 407 cells, the RVD is known to be attained by operation of the following channels in concert: volume-sensitive Cl^- channels (Kubo & Okada, 1992), Ca^{2+}-activated K^+ channels (Hazama & Okada, 1988), Ca^{2+}-permeable non-selective cation channels (Okada et al., 1990) and water channels (Kida et al., 1998). However, phloretin has been reported to enhance, but not suppress, Ca^{2+}-activated K^+ channels in other cell types (Koh et al., 1994; Gribkoff et al., 1996). Since a swelling-induced increase in cytosolic Ca^{2+}, which is known to be triggered by Ca^{2+} influx through non-selective cation channels in Intestine 407 cells (Okada et al., 1990), was still observed in the presence of phloretin in our preliminary fura-2 study in Intestine 407 cells (K. Dezaki, H.-T. Fan and Y. Okada, unpublished observations), it is unlikely that phloretin inhibits swelling-induced activation of Ca^{2+}-permeable non-selective cation

channels. Phloretin was reported to inhibit the aquaporin-3 (AQP3) water channel expressed in *Xenopus* oocytes (Ishibashi et al., 1994). As seen in Fig. 1, actually, the rate of osmotic swelling was found to be markedly suppressed by phloretin at 10 and 300 μM in Intestine 407 cells (Fan et al., 2000). However, the RVD was never blocked by phloretin at 10 μM. This result suggests that the phloretin-sensitive sub-type(s) of water channels is not essentially involved in the RVD mechanism.

At 30 to 300 μM, phloretin never inhibited Ca^{2+}-activated Cl^- currents in T84 cells (Fig. 15). These results are in good agreement with previous observations with 50 μM phloretin (Worrell & Frizzell, 1991). Ionomycin-induced activation of Ca^{2+}-dependent Cl^- currents persisted only for a short time but decayed soon even during persistent stimulation with ionomycin (Fig. 14). This decay may not be due to the decline of cytosolic Ca^{2+} level, because an increase in cytosolic Ca^{2+} was found to be sustained during stimulation with ionomycin (K. Dezaki, H.-T. Fan and Y. Okada, unpublished observations). A similar decay of Ca^{2+}-activated Cl^- currents before the cytosolic Ca^{2+} decline was found in equine tracheal smooth muscle cells and reported to be due to phosphorylation mediated by Ca^{2+}/calmodulin-dependent kinase II (CaMK II) (Wang & Kotlikoff, 1997). The present study showed that Ca^{2+}-activated Cl^- currents became reactivated when phloretin was applied after inactivation or rundown of the current (Fig. 15). The exact mechanism of phloretin-induced reactivation of the Ca^{2+}-activated Cl^- current is unknown. However, it is noted that phloretin enhanced the ionomycin-induced rise of intracellular Ca^{2+} level, although phloretin alone never affected the cytosolic Ca^{2+} concentration in

Intestine 407 cells (K. Dezaki, H.-T. Fan and Y. Okada, unpublished observations).

At 30 μM, phloretin exhibited no inhibitory effect on cAMP-activated CFTR Cl^- currents in both T84 cells (Fig. 17) and C127/CFTR cells (Fig. 21). However, at high concentrations (over 100 μM), phloretin suppressed preferentially inward components of cAMP-activated Cl^- currents (Figs. 18, 19 & 22). These results are in contrast to the previous observations of no detectable effect of 350 μM phloretin on CFTR Cl^- currents expressed in *Xenopus* oocytes (Schreiber et al., 1997). The activity of CFTR Cl^- channel is known to be dependent on phosphorylation by PKC (Tabcharani et al., 1991; Winpenny et al., 1995; Jia et al., 1997). Phloretin was reported to inhibit PKC (Gschwendt et al., 1984). However, an involvement of PKC in phloretin-induced suppression of cAMP-activated Cl^- currents is unlikely because: 1) the phloretin effect was voltage-dependent (Figs. 18, 19 & 22), 2) phloretin was ineffective when applied from the intracellular side (Fig. 20), and 3) a PKC inhibitor, calphostin C, failed to inhibit cAMP-activated Cl^- currents (Fig. 23).

At much lower concentrations, phloretin inhibited, in a voltage-independent manner, volume-sensitive Cl^- currents in three different cell types (Figs. 2, 4, 7, 8, 10 & 11). This effect should also be independent of PKC for the following reasons: 1) Phloretin failed to exert an inhibitory action when added to the intracellular solution (Fig. 9). 2) Volume-sensitive Cl^- currents were never affected by phloridzin (Fig. 12), which is known to act as a PKC inhibitor (Shoji et al., 1997). 3) In Intestine 407 cells, the activity of volume-sensitive Cl^- channel was found to be insensitive to non-

specific PKC blockers, polymixin B (Kubo & Okada, 1992) and H-7 (Okada et al., 1994). 4) A PKC-specific inhibitor, calphostin C, also never exhibited any inhibitory effect on volume-sensitive Cl^- currents (Fig. 13). Thus, it is most likely that phloretin exerts a direct inhibitory action from the extracellular side.

A part of the chemical formula of phloretin molecule resembles a stilbene-derivative Cl^- channel blocker (SITS or DIDS), especially in two benzene nuclei. However, the blocking mechanism of phloretin was distinct from that of SITS or DIDS which shows voltage-dependent (open-channel block-like) inhibition for volume-sensitive Cl^- channels in many cell types (see Okada, 1997). Since phloridzin was totally ineffective, the hydroxyl residue, at which D-glucose binds to a benzene nucleus of phloridzin (Table 2), would play an essential role in phloretin-induced blocking action. Phloretin has been reported to exhibit inhibitory effects on GLUT1 with IC_{50} of 50 to 60 μM (Kasahara & Kasahara, 1996) and on AQP3 at a concentration around 350 μM (Ishibashi et al., 1994). The present study showed that phloretin can inhibit volume-sensitive Cl^- channels at lower concentrations with IC_{50} of around 20 μM (Fig. 8). Although phloretin was shown to inhibit partially cAMP-activated Cl^- currents as well, much higher concentrations (IC_{50} of 252.2 μM for inward currents and 474.7 μM for outward currents; Fig. 19) were required. Thus, at lower concentrations, phloretin may serve as a specific blocker for volume-sensitive Cl^- channels, for which no specific blockers have been available so far. It is also expected that a more selective derivative of phloretin, if it were discovered, might offer a promising tool for purification of the volume-sensitive Cl^-

channel protein, the gene of which has not been cloned as yet (see Okada, 1997; Okada et al., 1998)

In summary, phloretin, a well-known inhibitor of glucose uniporters, inhibits volume-sensitive Cl^- channels in a voltage-independent manner at low concentrations (10 ~ 100 μM) in epithelial cells, whereas the drug partially inhibits cAMP-cativated CFTR Cl^- channels in a voltage-dependent manner at higher concentrations (over 100 μM). In contrast, phloretin never inhibited Ca^{2+}-activated Cl^- channels. It is concluded that phloretin is a novel type of Cl^- channel blocker, specifically for volume-sensitive Cl^- channels at concentrations below 100 μM.

REFERENCES

Arreola, J., J. E. Melvin, and T. Begenisich. Inhibition of Ca^{2+}-dependent Cl^- channels from secretory epithelial cells by low internal pH. *J. Membrane Biol.* 147: 95-104, 1995.

Betz, A. L., L. R. Drewes, and D. D. Gilboe. Inhibition of glucose transport into brain by phlorizin, phloretin and glucose analogues. *Biochim. Biophys. Acta* 406: 505-515, 1975.

Chang, H.-C., M. A. Kaetzel, D. J. Nelson, P. Hazarika, and J. R. Dedman. Antibody against a cystic fibrosis transmembrane conductance regulator-derived synthetic peptide inhibits anion currents in human colonic cell line T84. *J. Biol. Chem.* 267:8411-8416, 1992.

Cliff, W. H., and R. A. Frizzell. Separate Cl^- conductances activated by cAMP and Ca^{2+} in Cl^- secreting epithelial cells. *Proc. Natl. Acad. Sci. USA* 87: 4956-4960, 1990.

Duan, D., C. Winter, S. Cowley, J. R. Hume, and B. Horowitz. Molecular identification of a volume-regulated chloride channel. *Nature* 390: 417-421, 1997.

Echevarria, M., E. E. Windhager, and G. Frind. Selectivity of the renal collecting duct water channel aquaporin-3. *J. Biol. Chem.* 271: 25079-

25082, 1996.

Evans, M. G., and A. Marty. Calcium-dependent chloride currents in isolated cells from rat lacrimal glands. *J. Physiol. (London)* 378: 437-460, 1986.

Fan, H-T., H. Kida, S. Morishima, and Y. Okada. Phloretin inhibits a regulatory volume decrease in human epithelial cells. *In Control and Diseases of Sodium Dependent Transportation Proteins and Ion Channels* (Y. Suketa, ed.) Elsevier, Amsterdam, 2000 (in press).

Findlay, I., and O. H. Petersen. Acetylcholine stimulates a Ca^{2+}-dependent Cl^- conductance in mouse lacrimal acinar cells. *Pflügers Arch. – Eur. J. Physiol.* 403: 328-330, 1985.

Gribkoff, V. K., J. T. Lum-Ragan, C. G. Boissard, D. J. P. Munson, N. A. Meanwell, J. E. Starrett, E. S. Kozlowski, J. L. Romine, J. T. Trojnacki, M. C. Mckay, J. Zhong, and S. I. Dworetzky. Effects of channel modulators on cloned large-conductance calcium-activated potassium channels. *Mol. Pharmacol.* 50: 206-217, 1996.

Gschwendt, M., F. Horn, W. Kittstein, G. Furstenberger, E. Besenfelder, and F. Marks. Calcium and phospholipid-dependent protein kinase activity in mouse epidermis cytosol. Stimulation by complete and incomplete tumor promoters and inhibition by various compounds. *Biochem. Biophys. Res.*

Commun. 124: 63-68, 1984.

Hazama, A., H-T. Fan, I. Abdullaev, E. Maeno, S. Tanaka, Y. Ando-Akatsuka, and Y. Okada. Swelling-activated, cystic fibrosis transmembrane conductance regulator-augmented ATP release and Cl^- conductances in murine C127 cells. *J. Physiol. (London)* S23: 1-11, 2000.

Hazama, A., A. Miwa, T. Miyoshi, T. Shimizu, and Y. Okada. ATP release from swollen or CFTR-expressing epithelial cells. In *Cell Volume Regulation: The Molecular Mechanism and Volume Sensing Machinery* (Y. Okada, ed.) Elsevier, Amsterdam, 1998.

Hazama, A., and Y. Okada. Ca^{2+} sensitivity of volume-regulatory K^+ and Cl^- channels in cultured human epithelial cells. *J. Physiol. (London)* 402: 687-702, 1988.

Hazama, A., T. Shimizu, Y. Ando-Akatsuka, S. Hayashi, S. Tanaka, E. Maeno, and Y. Okada. Swelling-activated, CFTR-independent ATP release from a human epithelial cell line: Lack of correlation with volume-sensitive Cl^- channels. *J. Gen. Physiol.* 114: 525-533, 1999.

Ishibashi, K., S. Sasaki, K. Fushimi, S. Uchida, M. Kuwahara, H. Sato, T. Furukawa, K. Nakajima, Y. Yamaguchi, T. Gojobori, and F. Marumo. Molecular cloning and expression of a member of the aquaporin family with permeability to glycerol and urea in addition to water

expressed at the basolateral membrane of kidney collecting duct cells. *Proc. Natl. Acad. Sci. USA* 91: 6269-6273, 1994.

Jia, Y., C. J. Mathews, and J. W. Hanrahan. Phosphorylation by protein kinase C is required for acute activation of cystic fibrosis transmembrane conductance regulator by protein kinase A. *J. Biol. Chem.* 272: 4978-4984, 1997.

Kasahara, T., and M. Kasahara. Expression of the rat GLUT1 glucose transporter in the yeast. *Saccharomyces cerevisiae. Biochem. J.* 315: 177-182, 1996.

Kida, H., S. Morishima, S. Ueda, T. Miyoshi, T. Chiba, and Y. Okada. The role of water channels in osmotic water flow and cell volume regulation in a human small intestine epithelial cell line. *Jpn. J. Physiol.* 48: S49, 1998 (Abstract).

Kobayashi, E., H. Nakano, M. Morimoto, and T. Tamaoki. Calphostin C (UCN-1028C), a novel microbial compound, is a highly potent and specific inhibitor of protein kinase C. *Biochem. Biophys. Res. Commun.* 159: 548-553, 1989.

Kobori, M., H. Shinmoto, T. Tsushida, and K. shinohara. Phloretin-induced apoptosis in B16 melanoma 4A5 cells by inhibition of glucose transmembrane transport. *Cancer Letters* 119: 207-212, 1997.

Koh, D. S., G. Reid, and W. Vogel. Activating effect of the flavonoid phloretin on Ca^{2+}-activated K^+ channels in myelinated nerve fibers of *Xenopus laevis*. *Neurosci. Lett.* 165: 167-170, 1994.

Krause, K.-H., and M. J. Welsh. Voltage-dependent and Ca^{2+}-activated ion channels in human neutrophils. *J. Clin. Invest.* 85: 491-498, 1990.

Krupka, R. M. Asymmetrical binding of phloretin to the glucose transport system of human erythrocytes. *J. Membrane Biol.* 83: 71-80, 1985.

Kubo, M., and Y. Okada. Volume-regulatory Cl^- channel currents in cultured human epithelial cells. *J. Physiol. (London)* 456: 351-371, 1992.

Kunzelmann, K., R. Kubitz, M. Grolik, R. Warth, and R. Greger. Small-conductance Cl^- channels in HT_{29} cells: activation by Ca^{2+}, hypotonic cell swelling and 8-Br-cGMP. *Pflügers Arch. – Eur. J. Physiol.* 421: 238-246, 1992.

Kunzelmann, K., and R. Schreiber. CFTR, a regulator of channels. *J. Membrane Biol.* 168: 1-8, 1999.

Lang, F. *Cell Volume Regulation: Contrib. Nephrol.* Basel, Karger, vol 123, 1998.

Liu, Y., S. Oiki, T. Tsumura, T. Shimizu, and Y. Okada. Glibenclamide blocks volume-sensitive Cl^- channels by dual mechanisms. *Am. J. Physiol.* 275: C343-C351, 1998.

Loo, D. D. F., B. A. Hirayama, A-K. Meinild, G. Chandy, T. Zeuthen, and E. M. Wright. Passive water and ion transport by cotransporters. *J. Physiol. (London)* 518: 195-292, 1999.

McCarty, N. A., and R. G. O'Neil. Calcium signaling in cell volume regulation. *Physiol. Rev.* 72: 1037-1061, 1992.

Merlin, D., L. Jiang, G. R. Strohmeier, A. Nusrat, S. L. Alper, W. I. Lencer, and J. L. Madara. Distinct Ca^{2+}- and cAMP-dependent anion conductances in the apical membrane of polarized T84 cells. *Am. J. Physiol.* 275: C484-C495, 1998.

Morishima, S., H. Kida, S. Ueda, T. Chiba, and Y. Okada. Water movement during cell volume regulation. In *Cell Volume Regulation: The Molecular Mechanism and Volume Sensing Machinery* (Y. Okada, ed.) Elsevier, Amsterdam, 1998.

Okada, Y. Volume expansion-sensing outward-rectifier Cl^- channel: fresh start to the molecular identity and volume sensor. *Am. J. Physiol.* 273: C755-C789, 1997.

Okada, Y. *Cell Volume Regulation: The Molecular Mechanism and Volume Sensing Machinery* Elsevier, Amsterdam, 1998.

Okada, Y., A. Hazama, and W.-L. Yuan. Stretch induced activation of Ca^{2+}-permeable ion channels is involved in the volume regulation of hypotonically swollen epithelial cells. *Neurosci. Res.* 12: S5-S13, 1990.

Okada, Y., M. Kubo, S. Oiki, C. C. Petersen, M. Tominaga, A. Hazama, and S. Morishima. Properties of volume-sensitive Cl^- channels in a human epithelial cell. *Jpn. J. Physiol.* 44: S31-S35, 1994.

Okada, Y., S. Oiki, A. Hazama, and S. Morishima. Criteria for the molecular identification of the volume-sensitive outwardly rectifying Cl^- channel. *J. Gen. Physiol.* 112: 365-367, 1998.

Pedersen, S. F., J. Prenen, G. Droogmans, E. K. Hoffman, and B. Nilius. Separate swelling- and Ca^{2+} activated anion currents in ehrlich ascites tumor cells. *J. Membrane Biol.* 163: 97-110, 1998.

Prevarskaya, N., R. Skryma, P. Vacher, L. B. Bepoldin, M. F. Odessa, J. Rivel, F. S. Galli, J. Guerin, and L. D. Barbe. Gonadotropin-releasing hormone induced Ca^{2+} influx in nonsecreting pitutary adenoma cells: role of voltage-dependent Ca^{2+} channels and protein kinase C. *Mol. Cell Neurosci.* 5: 699-708, 1994.

Rozmahel, R., M. Wilschanski, A. Matin, S. Plyte, M. Oliver, W. Auerbach, A. Moore, J. Forstner, P. Durie, J. Nadeau, C. Bear, and L-C. Tsui. Modulation of disease severity in cystic fibrosis transmembrane conductance regulator deficient mice by a secondary genetic factor. *Nature Genetics* 12: 280-287, 1996.

Sahagian, B. M. Active glucose uptake by strips of guinea pig intestine; competitive inhibition by phlorhizin and phloretin. *Can. J. Biochem.* 43: 851-858, 1965.

Schreiber, R., R. Greger, R. Nitschke, and K. Kunzelmann. Cystic fibrosis transmembrane conductance regulator activates water conductance in *Xenopus* oocytes. *Pflügers Arch. – Eur. J. Physiol.* 434: 841-847, 1997.

Schwiebert, E. M., D. J. Benos, M. E. Egan, M. J. Stutts, and W. B. Guggino. CFTR is a conductance regulator as well as a chloride channel. *Physiol. Rev.* 79: S145-S166, 1999.

Seshadri, T. R. Biochemistry of natural pigments. *Ann. Rev. Biochem.* 20: 487-512, 1951.

Shoji, T, M. Kobori, H. Shinomoto, M. Tanabe, and T. Tsushida. Progressive effects of phloridzin on melanogenesis in B16 mouse melanoma cells. *Biosci. Biotech. Biochem.* 61: 1963-1967, 1997.

Strange, K., F. Emma, and P. S. Jackson. Cellular and molecular physiology of volume-sensitive anion channels. *Am. J. Physiol.* 270: C711-C7730, 1996.

Tabcharani, J. A., X. B. Chang, J. R. Riordan, and J. W. Hanrahan. Phosphorylation-regulated Cl^- channel in CHO cells stably expressing the cystic fibrosis gene. *Nature* 352: 628-631, 1991.

Taleb, O., P. Feltz, J.-L. Bossu, and A. Feltz. Small-conductance chloride channels activated by calcium on cultured endocrine cells from mammalian pars intermedia. *Pflügers Arch. – Eur. J. Physiol.* 412: 641-646, 1988.

Tilly, B. C., M. J. Edixhoven, N. V. D. Berghe, A. G. M. Bot, and H. R. D. Jonge. Ca^{2+} mobilizing hormones potentiate hypotonicity-induced activation of ionic conductances in intestine 407 cells. *Am. J. Physiol.* 267: C1271-C1278, 1994.

Tominaga, M., T. Tominaga, A. Miwa, and Y. Okada. Volume-sensitive chloride channel activity does not depend on endogenous P-glycoprotein. *J. Biol. Chem.* 270: 27887-27893, 1995.

Tsumura, T., S. Oiki, S. Ueda, M. Okuma, and Y. Okada. Sensitivity of volume-sensitive Cl^- conductance in human epithelial cells to extracellular nucleotides. *Am. J. Physiol.* 271: C1872-C1878, 1996.

Wagner, J. A., A. L. Cozens, H. Schulman, D. C. Gruenert, L. Stryer, and P. Gardner. Activation of chloride channels in normal and cystic fibrosis airway epithelial cells by multifunctional calcium/calmodulin-dependent protein kinase. *Nature* 349: 793-796, 1992.

Wang, Y.-X., and M. I. Kotlikoff. Inactivation of calcium-activated chloride channels in smooth muscle by calcium/calmodulin-dependent protein kinase. *Proc. Natl. Acad. Sci. USA* 94: 14918-14923, 1997.

Wang, Z., T. Mitsuiye, S. Rees, and A. Noma. Regulatory volume decrease of cardiac myocytes induced by ß-adrenergic activation of the Cl^- channel in guinea pig. *J. Gen. Physiol.* 110: 73-82, 1997.

Welsh, M. J. Single apical membrane anion channels in primary cultures of canine tracheal epithelium. *Pflügers Arch. – Eur. J. Physiol.* 407: S116-S122, 1986.

Winpenny, J. P., H. L. McAlroy, M. A. Gray, and B. E. Argent. Protein kinase C regulates the magnitude and stability of CFTR currents in pancreatic duct cells. *Am. J. Physiol.* 268: C823-C828, 1995.

Worrell, R. T., A. G. Butt, W. H. Cliff, and A. Frizzell. A volume-sensitive chloride conductance in human colonic cell line T84. *Am. J. Physiol.* 256: C1111-C1119, 1989.

Worrell, R. T., and R. A. Frizzell. CaMKII mediates stimulation of cholide conductance by calcium in T84 cells. *Am. J. Physiol.* 260: C877-C882, 1991.

Zygmunt, A. C., and W. R. Gibbons. Calcium-activated chloride current in rabbit ventricular myocytes. *Cir. Res.* 68: 424-437, 1991.

Figure Legend

Figure 1. Volume regulation of Intestine 407 cells after exposure to hypotonic solution in the absence (control) or presence of phloretin (10 or 300 μM). Cell volume was measured by high-speed automatic image analysis. (Data from Fan et al., 2000).

Figure 2. Effects of extracellular phloretin on volume-sensitive whole-cell Cl^- currents in T84 cells. *A*: typical record before and after osmotic cell swelling in the absence or presence of phloretin at different concentrations (indicated by horizontal lines) in bath solution during application of alternating pulses from 0 to ±40 mV or of step pulses from –100 mV to +100 mV in 20-mV increments (at *a*, *b* & *c*). *B*: expanded traces of current responses (*a*, *b* & *c* in *A*) to step pulses, the protocol of which is shown in *inset,* in the absence (*a*) or presence of phloretin at 30 μM (*b*) or 300 μM (*c*).

Figure 3. Effects of changes in the extracellular Cl^- concentration on the current-voltage relationship measured by ramp voltage clamp in T84 cells. Ramp pulses from –100 mV to +100 mV were applied after the steady current activation was observed. Cl^- gradients are indicated on current traces in mM/mM.

Figure 4. Effects of extracellular phloretin on the current-voltage relationship of volume-sensitive Cl^- currents in T84 cells. Upper panel

shows the instantaneous current-voltage curves, and the steady-state current-voltage curves are shown in the bottom. Each symbol represents the mean current (with the SEM: *vertical bars*) of 8 to 12 experiments performed in the absence (control: *filled circles*) or presence of phloretin at 30 μM (*open circles*) or 300 μM (*squares*). * indicates significant differences ($P<0.05$) from control experiments. ** indicates statistical significance ($P<0.05$) between the values of experiments in the presence of phloretin at 30 μM and 300 μM.

Figure 5. Voltage independence of phloretin-induced inhibition of volume-sensitive Cl^- currents (top: instantaneous currents; bottom: steady-state currents) in T84 cells. Each symbol represents the ratio of the current density in the presence of 30 μM phloretin to that in the absence of phloretin (control values in Figure 4).

Figure 6. Effects of phloretin on depolarization-induced inactivation kinetics of volume-sensitive Cl^- currents in T84 cells. *A*: inactivation time courses during application of steps to +100 mV in the absence (*control*) or presence of 30 μM phloretin. Red curves are biexponential fits. *B*: fast (τ_f) and slow (τ_s) time constants for inactivation of volume-sensitive Cl^- currents in the absence (*control*) or presence of 30 μM phloretin at +100 mV (means ± SEM, n=8). Differences between values of control experiments and those with phloretin are not statistically significant ($P > 0.05$).

Figure 7. Effects of extracellular phloretin on volume-sensitive whole-cell Cl^- currents in Intestine 407 cells. *A*: typical record before and after osmotic cell swelling in the absence or presence of phloretin at different concentrations (indicated by horizontal lines) in bath solution during application of alternating pulses from 0 to ±40 mV. *B*: typical traces of steady current responses to step pulses of which protocol is shown in *inset* in the absence (*control*) or presence of phloretin at 3, 30 or 300 μM.

Figure 8. Concentration-response curve for the inhibition of volume-sensitive Cl^- currents by phloretin at +60 mV. Each symbol represents the mean ± SEM (n=7 to 11). Data were fitted to a sigmoidal relation with IC_{50} of 20.4 ± 5.9 μM and n=1.3.

Figure 9. Effects of intracellular phloretin (300 μM in pipette solution) on the current-voltage relationship of volume-sensitive Cl^- currents in Intestine 407 cells. Upper panel shows the instantaneous current-voltage curves, and the steady-state current-voltage curves are shown in the bottom. Each symbol represents the mean current (with the SEM: *vertical bars*) of 24 to 30 experiments performed in the absence (control: *open squares*) or presence of intracellular phloretin (300 μM: *filled squares*). Differences between values in the absence and those in the presence of intracellular phloretin are statistically insignificant ($P > 0.05$) at each potential.

Figure 10. Effects of extracellular phloretin on volume-sensitive whole-cell Cl^- currents in C127/CFTR cells. *A*: the traces of steady current responses

to step pulses, the protocol of which is shown in *inset*, in the absence (*control*) or presence of phloretin at 3, 30 or 300 μM. *B*: Effects of changes in the extracellular Cl^- concentration on current-voltage curves measured by ramp voltage clamp. Ramp pulses from –100 mV to +100 mV were applied after the steady current activation was observed. Cl^- gradients are indicated on current traces in mM/mM.

Figure 11. Effects of extracellular phloretin on the current-voltage relationship of volume-sensitive Cl^- currents in C127/CFTR cells. Upper panel shows the instantaneous current-voltage curves, and the steady-state current-voltage curves are shown in the bottom. Each symbol represents the mean current (with the SEM: *vertical bars*) of 8 to 10 experiments performed in the absence (control: *squares*) or presence of phloretin at 30 μM (*open circles*) or 300 μM (*filled circles*). * indicates significant differences ($P<0.05$) from control experiments. ** indicates statistical significance ($P<0.05$) between the values of experiments in the presence of phloretin at 30 μM and 300 μM.

Figure 12. Effects of extracellular phloridzin on whole-cell volume-sensitive Cl^- currents in Intestine 407 cells. *A*: typical record before and after osmotic cell swelling in the absence or presence of 100 μM phloridzin (indicated by horizontal lines) in bath solution during the application of alternating pulses from 0 to ±40 mV or of step pulses from –100 mV to +100 mV in 20-mV increments (at *a* & *b*). *B*: expanded traces of current responses (*a* & *b* in *A*) to step pulses of which protocol is shown in *inset* in

the absence (*a*) or presence of phloridzin at 100 μM (*b*). *C*: instantaneous and steady-state current-voltage curves measured in the absence (control: *open circles*) or presence of 100 μM phloridzin (*filled circles*). Differences between values of control experiments and those with phloridzin are not statistically significant ($P > 0.05$).

Figure 13. Effects of calphostin C, a specific inhibitor of protein kinase C, on volume-sensitive whole-cell Cl^- currents in Intestine 407 cells. *A*: typical record before and after osmotic cell swelling in the absence or presence of 500 nM calphostin C (indicated by horizontal lines) in bath solution during application of alternating pulses from 0 to ±40 mV or of step pulses from –100 mV to +100 mV in 20-mV increments (at *a* & *b*). *B*: expanded traces of current responses (*a* & *b* in *A*) to step pulses of which protocol is shown in *inset* in the absence (*a*) or presence of calphostin C at 500 nM (*b*). *C*: instantaneous and steady-state current-voltage curves measured in absence (control: *open squares*) or presence of 500 nM calphostin C (*filled squares*). Differences between values of control experiments and those with calphostin C are not statistically significant ($P > 0.05$).

Figure 14. Ca^{2+}-activated whole-cell Cl^- currents induced by a Ca^{2+} ionophore, ionomycin (2.5 μM), in T84 cells. *A*: typical record of the ionomycin-induced whole-cell current before and after changing the extracellular Cl^- concentration during the application of alternating pulses from 0 to ±40 mV or of step pulses from –100 mV to +100 mV in 20-mV increments (at *a* & *b*). *B*: expanded traces of current responses (*a* & *b* in *A*)

to step pulses, the protocol of which is shown in *inset,* in the bath solution containing 19 mM (*a*) or 121 mM Cl^- ions (*b*). *C*: current-voltage curves under different Cl^- gradient. The reversal potential was shifted by 31.1 ± 0.9 mV when the bath Cl^- concentration was reduced from 121 mM to 19 mM.

Figure 15. Effects of extracellular phloretin on Ca^{2+}-activated whole-cell Cl^- currents in T84 cells. *A*: typical record of the ionomycin-induced whole-cell Cl^- currents in the absence or presence of 30 μM phloretin (indicated by horizontal lines) in bath solution during the application of alternating pulses from 0 to ±80 mV or of step pulses from –100 mV to +100 mV in 20-mV increments (at *a* & *b*). *B*: expanded traces of current responses (*a* & *b* in *A*) to step pulses, the protocol of which is shown in *inset,* in the absence (*a*) or presence of phloretin at 30 μM (*b*). *C*: effects of phloretin on the current density at –80 mV or +80 mV. Data were shown by mean ± SEM (n=7). Differences between values of control and those with phloretin are statistically significant (*$P < 0.05$ or ** $P < 0.01$).

Figure 16. Comparison of ionomycin-induced activation of Ca^{2+}-dependent whole-cell Cl^- currents in T84 cells between before and after preincubating with 30 μM phloretin. *A*: typical record of the ionomycin-induced whole-cell Cl^- currents in the absence (*left*) or presence (*right*) of 30 μM phloretin (indicated by horizontal lines) in bath solution during application of ramp pulses from 0 to ±80 mV (the protocol indicated in *inset*). *B*: effects of pretreatment with phloretin on the current density at –80 mV or +80 mV.

Data were shown by mean ± SEM (n=6 or 7). Differences between values of control and those with phloretin are statistically insignificant ($P > 0.05$).

Figure 17. Effects of extracellcular 30 μM phloretin on cAMP-activated whole-cell Cl^- currents in T84 cells. *A*: typical record at a holding potential of –20 mV before and after application of a cocktail of forskolin (10 μM), dbcAMP (500 μM) and IBMX (400 μM) in the absence or presence of 30 μM phloretin (indicated by horizontal lines) in bath solution during application of alternating pulses from 0 mV to –84 mV or of step pulses from –100 mV to +100 mV in 20-mV increments (at *a* & *b*). *B*: expanded traces of current responses (*a* & *b* in *A*) to step pulses, the protocol of which is shown in *inset*, in the absence (*a*) or presence of 30 μM phloretin (*b*). *C*: current-voltage curves measured in the absence (control: *open circles*) or presence of 30 μM phloretin (*filled circles*). Differences between values of control and those with phloretin are statistically insignificant ($P > 0.05$).

Figure 18. Effects of extracellcular 300 μM phloretin on cAMP-activated whole-cell Cl^- currents in T84 cells. *A*: typical record at a holding potential of –20 mV before and after application of a cocktail of forskolin (10 μM), dbcAMP (500 μM) and IBMX (400 μM) in the absence or presence of 300 μM phloretin (indicated by horizontal lines) in bath solution during application of alternating pulses from 0 mV to –84 mV or of step pulses from –100 mV to +100 mV in 20-mV increments (at *a* & *b*). *B*: expanded traces of current responses (*a* & *b* in *A*) to step pulses, the protocol of

which is shown in *inset,* in the absence (*a*) or presence of 300 μM phloretin (*b*). *C*: current-voltage curves measured in the absence (control: *open circles*) or presence of 30 μM phloretin (*filled circles*). * indicates significant differences ($P < 0.05$) from control experiments.

Figure 19. Concentration-response curves for the inhibition of cAMP-activated Cl^- currents by phloretin at –60 mV and +60 mV in T84 cells. Each symbol represents the mean ± SEM (n=7 to 13). Data were fitted to a sigmoidal relation with IC_{50} of 474.7 ± 24.5 μM and *n* of 3.2 at +60 mV and IC_{50} of 252.0 ± 20.7 μM and *n* of 1.5 at –60 mV. Differences between data at +60 mV and –60 mV are significant ($P < 0.05$) at 100 and 300 μM phloretin.

Figure 20. Effects of intracellular phloretin (300 μM in pipette solution) on the current-voltage relationship of cAMP-activated Cl^- currents in T84 cells. Each symbol represents the mean current of 8 or 9 experiments with the SEM of the mean (*vertical bar*). Differences between values in the absence (control: *open circles*) and those in the presence of phloretin (*filled circles*) are statistically insignificant ($P > 0.05$) at each potential.

Figure 21. Effects of extracellular phloretin on cAMP-activated whole-cell Cl^- currents in C127/CFTR cells. *A*: typical record at a holding potential of 0 mV before and after application of a cocktail of forskolin (10 μM), dbcAMP (500 μM) and IBMX (400 μM) in the absence or presence of 30 μM phloretin (indicated by horizontal lines) in bath solution during

application of ramp pulses from –80 mV to +80 mV or of step pulses from –100 mV to +100 mV in 20-mV increments (at *a* & *b*). *B*: expanded traces of current responses (*a* & *b* in *A*) to step pulses, the protocol of which is shown in *inset*, in the absence (*a*) or presence of 30 μM phloretin (*b*). *C*: current-voltage curves measured in the absence (control: *open circles*) or presence of 30 μM phloretin (*filled circles*). Differences between values in the absence and those in the presence of phloretin are statistically insignificant ($P > 0.05$) at each potential.

Figure 22. Effects of extracellular phloretin on cAMP-activated whole-cell Cl^- currents in C127/CFTR cells. *A*: typical record at a holding potential of 0 mV before and after application of a cocktail of forskolin (10 μM), dbcAMP (500 μM) and IBMX (400 μM) in the absence or presence of 300 μM phloretin (indicated by horizontal lines) in bath solution during application of ramp pulses from –80 mV to +80 mV or of step pulses from –100 mV to +100 mV in 20-mV increments (at *a* & *b*). *B*: expanded traces of current responses (*a* & *b* in *A*) to step pulses, the protocol of which is shown in *inset*, in the absence (*a*) or presence of 300 μM phloretin (*b*). *C*: current-voltage curves measured in the absence (control: *open circles*) or presence of 300 μM phloretin (*filled circles*). Differences between values in the absence and those in the presence of phloretin are statistically significant ($P < 0.05$) at each potential.

Figure 23. Effects of calphostin C on cAMP-activated whole-cell Cl^- currents in C127/CFTR cells. *A*: typical record at a holding potential of 0

mV before and after application of a cocktail of forskolin (10 μM), dbcAMP (500 μM) and IBMX (400 μM) in the absence or presence of 500 nM calphostin C (indicated by horizontal lines) in bath solution during application of alternating pulses from –40 to +40 mV or of step pulses from –100 mV to +100 mV in 20-mV increments (at *a* & *b*). *B*: expanded traces of current responses (*a* & *b* in *A*) to step pulses, the protocol of which is shown in *inset,* in the absence (a) or presence of calphostin C at 500 nM (*b*). *C*: current-voltage curves measured in the absence (control: *open squares*) or presence of 500 nM calphostin C (*filled squares*). Differences between values in the absence and those in the presence of calphostin C are statistically insignificant ($P > 0.05$) at each potential.

Table 1. Phenotypical characteristics of the three types of Cl^- channel

	Volume-sensitive (CLC-3?)	Ca^{2+}-activated (CLCA?)	cAMP-activated (CFTR)
I-V relationship	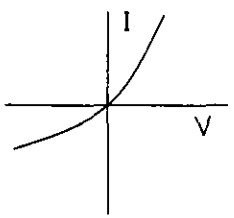	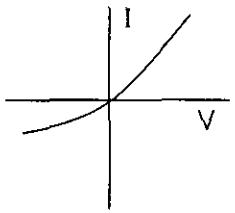	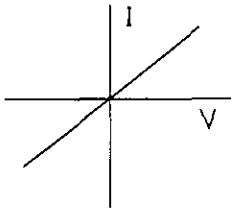
Single-channel conductance	15~75 pS	1~3 pS	8~10 pS
Voltage and time dependence	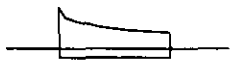	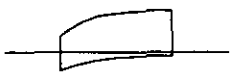	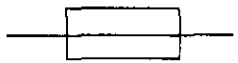
Anion selectivity	$I^- > Br^- > Cl^-$	$I^- > Br^- > Cl^-$	$Br^- > Cl^- > I^-$
Activator	Osmotic swelling	Intracellular Ca^{2+}	Intracellular cAMP
Blockers	SITS, DIDS, NPPB, DPC, 9AC, Tamoxifen, Glibenclamide, NFA	SITS, DIDS, NPPB, NFA, Tamoxifen, Glibenclamide	DPC, 9AC, Glibenclamide
T84 cells	+	+	+
Intestine 407 cells	+	–	–
C127/CFTR cells	+	+	+

+: expression -: no expression

Table 2. Chemical structures of phloretin and phloridzin

	Phloretin	Phloridzin
	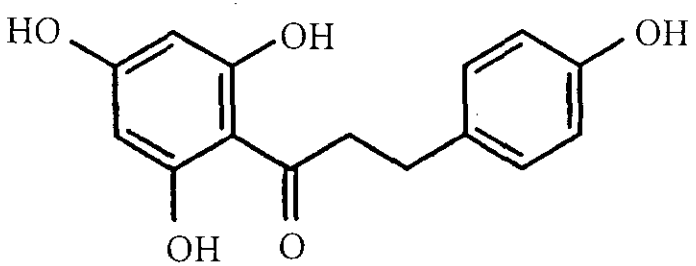	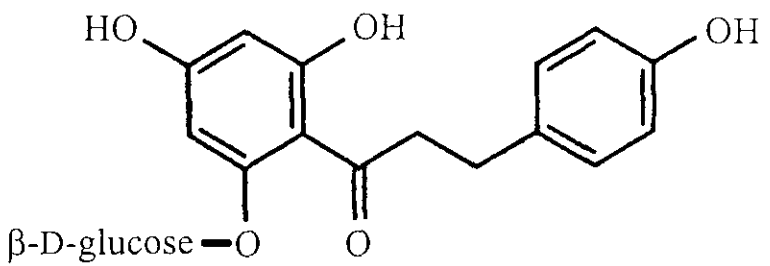
M.W.	274.27	436.42
Inhibitor for	Glucose uniporter (Glut) Water channel (AQP) Protein kinase C (PKC)	Na^+-glucose symporter (SGLT) PKC

Fig. 1

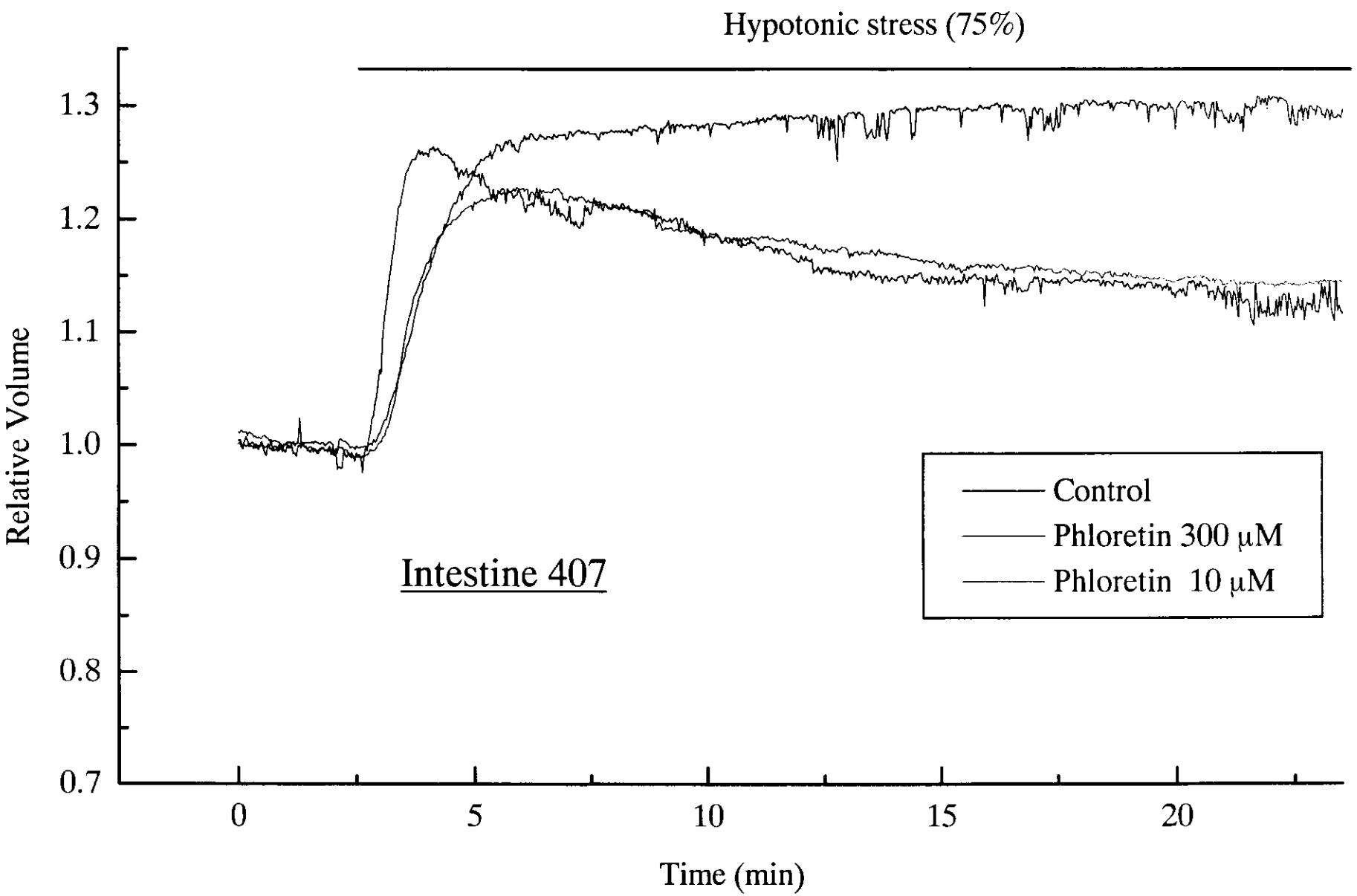
Hypotonic stress (75%)
Relative Volume
1.3
1.2
1.1
1.0
0.9
0.8
0.7
0
5
10
15
20
Time (min)
Intestine 407
Control
Phloretin 300 μM
Phloretin 10 μM

Fig. 2

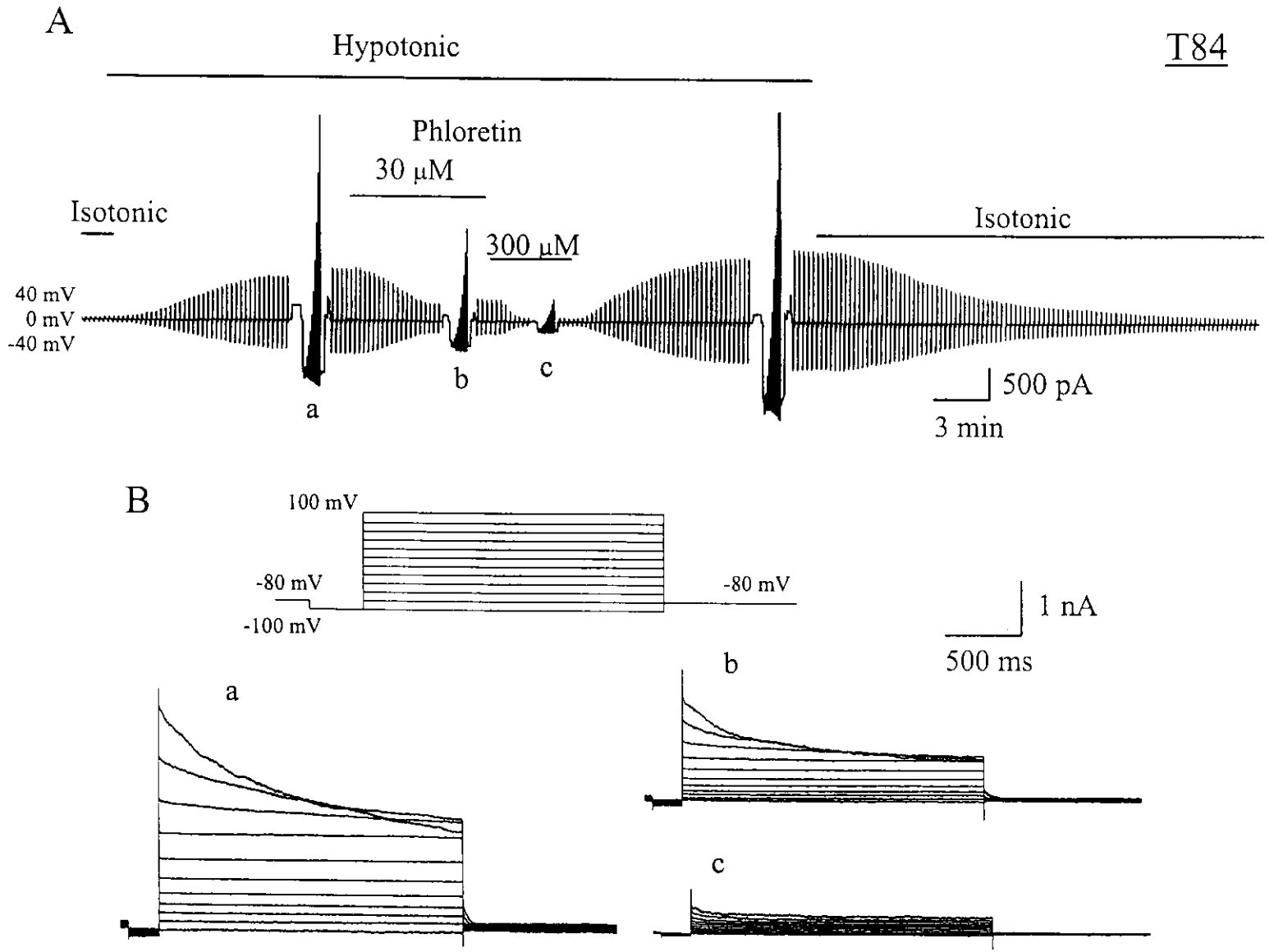
A
Hypotonic
T84
Phloretin
30 μM
Isotonic
300 μM
Isotonic
40 mV
0 mV
-40 mV
a
b
c
500 pA
3 min
B
100 mV
-80 mV
-80 mV
-100 mV
1 nA
500 ms
a
b
c

Fig. 3

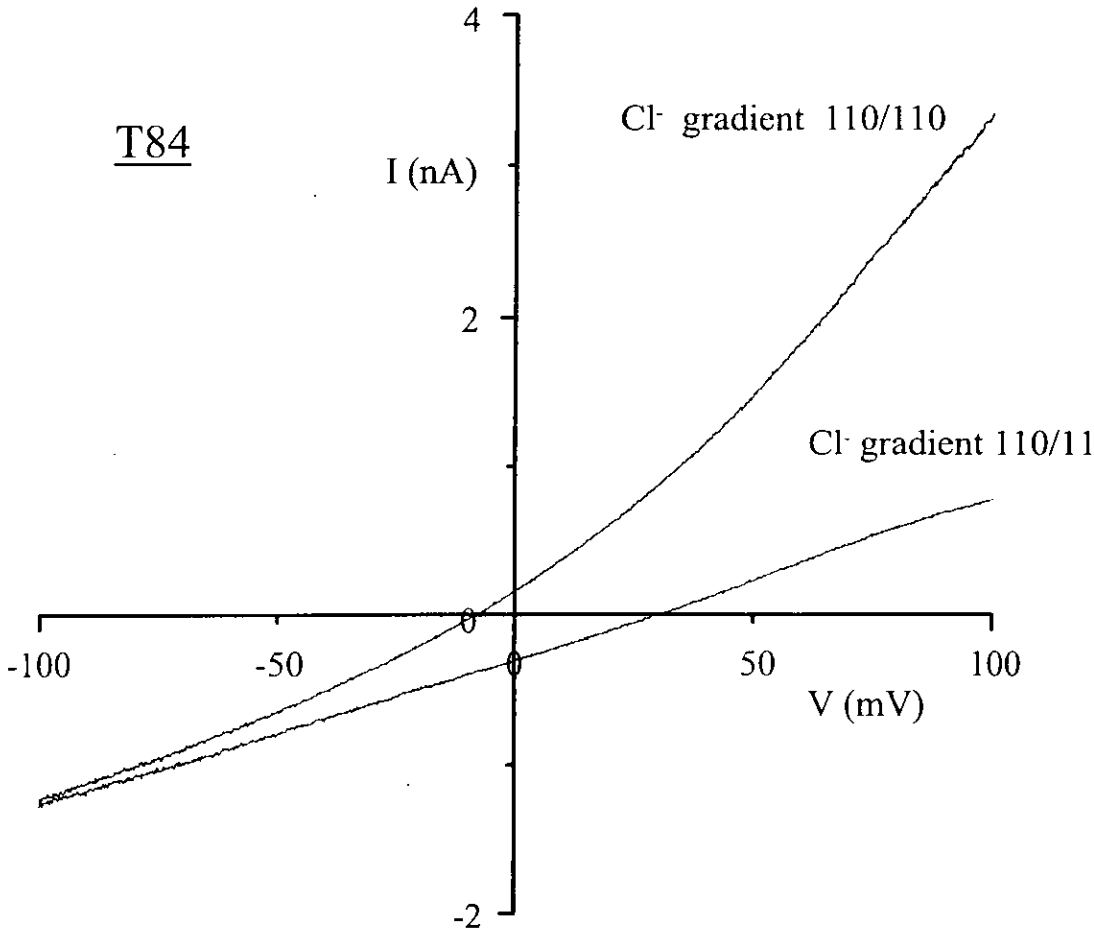
T84
I (nA)
4
2
0
-2
-100
-50
50
100
V (mV)
Cl- gradient 110/110
Cl- gradient 110/11

Fig. 4

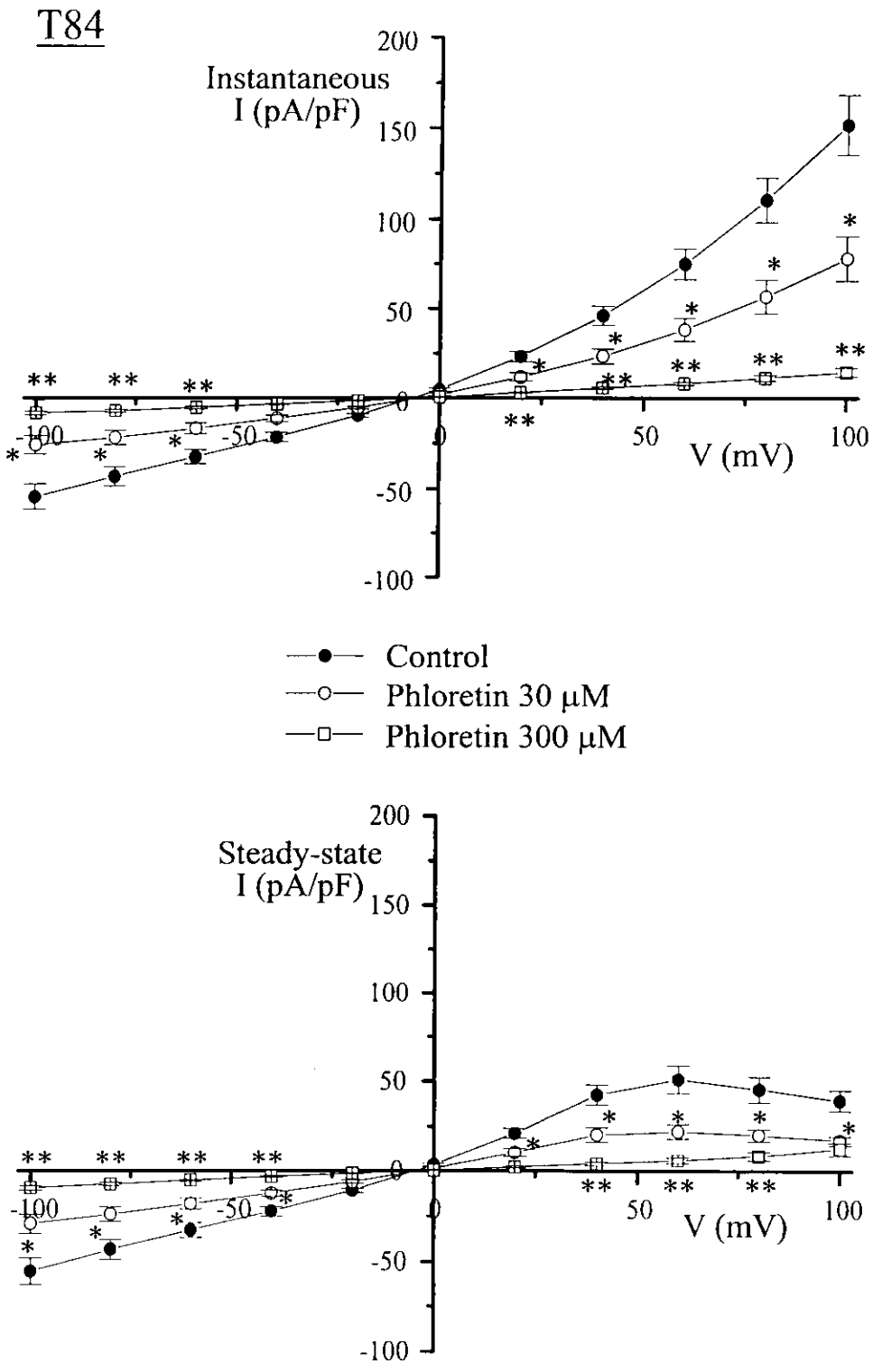
T84
Instantaneous
I (pA/pF)
200
150
100
50
0
-50
-100
-100
-50
50
100
V (mV)
Control
Phloretin 30 μM
Phloretin 300 μM
Steady-state
I (pA/pF)
200
150
100
50
0
-50
-100
-100
-50
50
100
V (mV)

Fig. 5

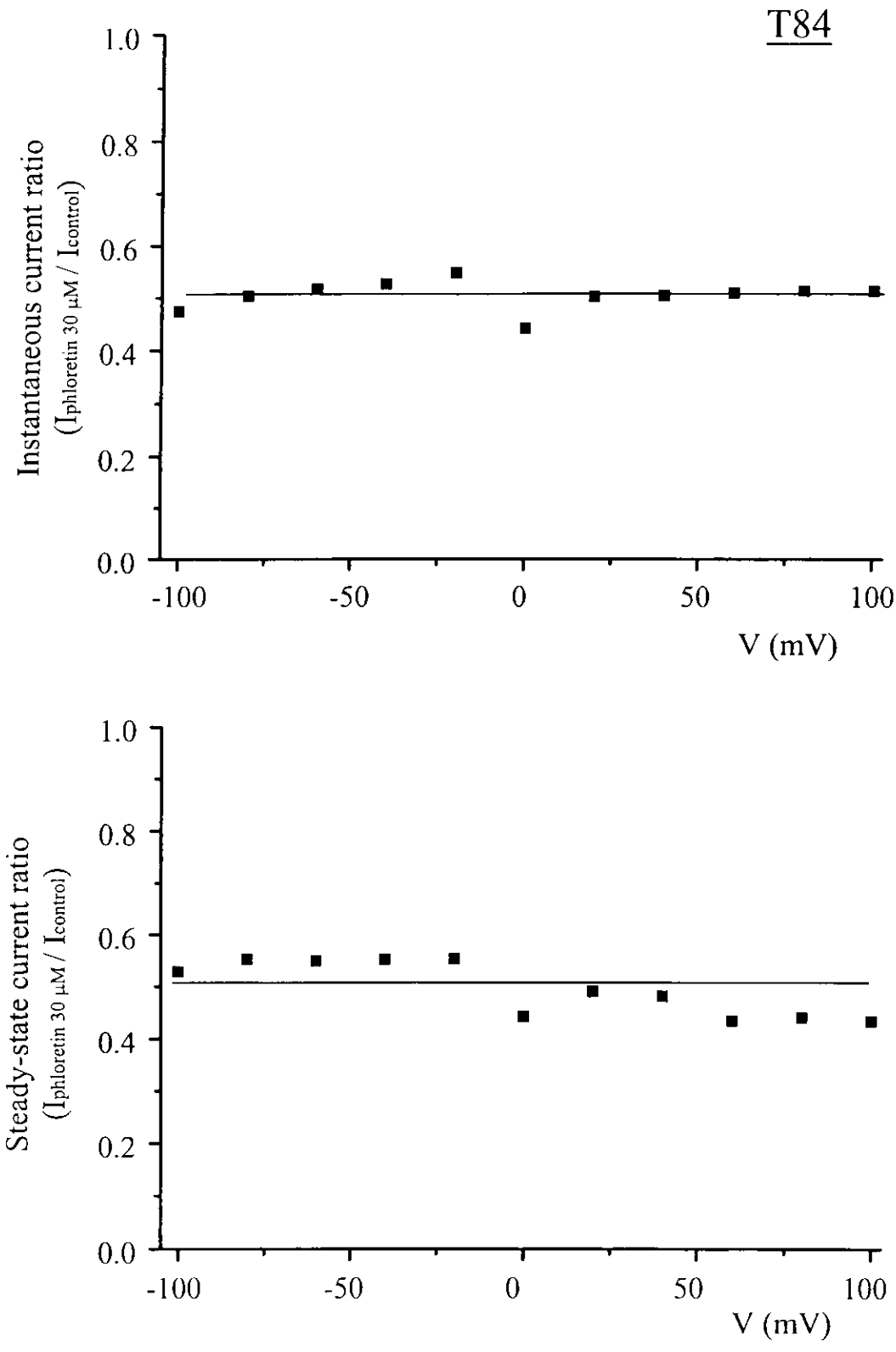
T84
Instantaneous current ratio
(Iphloretin 30 μM / Icontrol)
1.0
0.8
0.6
0.4
0.2
0.0
-100
-50
0
50
100
V (mV)
Steady-state current ratio
(Iphloretin 30 μM / Icontrol)
1.0
0.8
0.6
0.4
0.2
0.0
-100
-50
0
50
100
V (mV)

Fig. 6

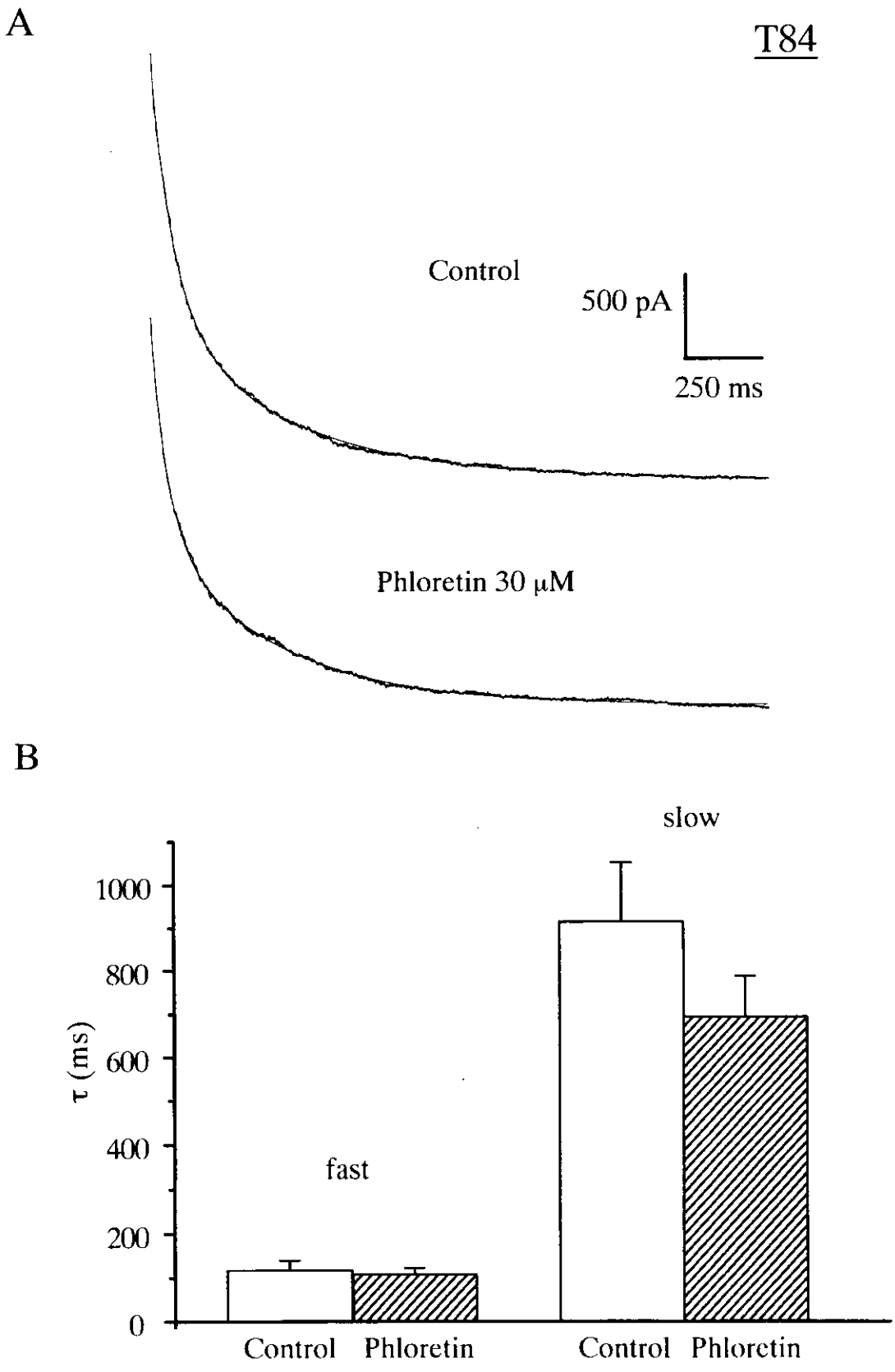
A
T84
Control
500 pA
250 ms
Phloretin 30 μM
B
slow
fast
τ (ms)
1000
800
600
400
200
0
Control
Phloretin
Control
Phloretin

Fig. 7

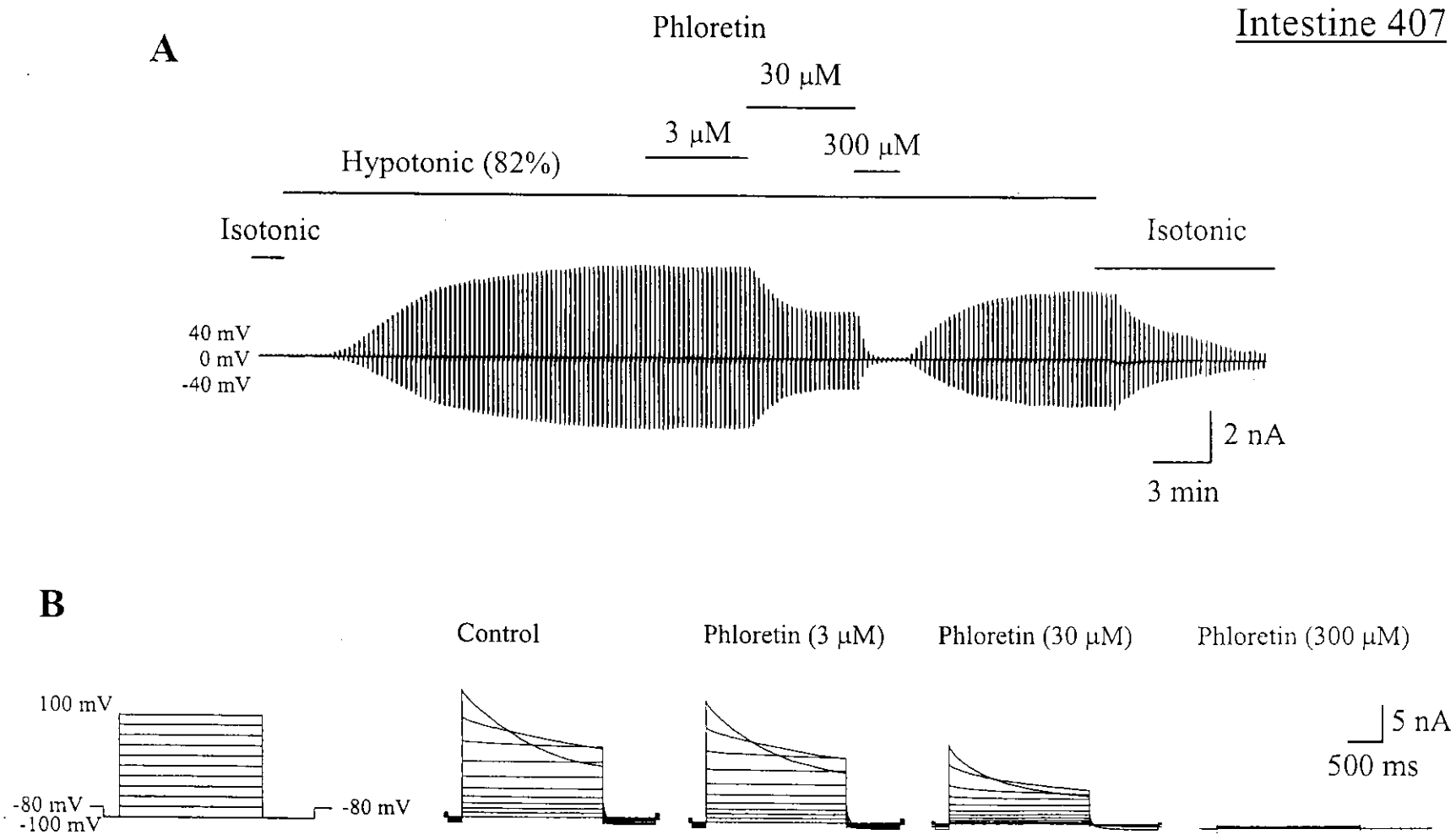
A
Intestine 407
Phloretin
30 μM
3 μM
300 μM
Hypotonic (82%)
Isotonic
Isotonic
40 mV
0 mV
-40 mV
2 nA
3 min
B
Control
Phloretin (3 μM)
Phloretin (30 μM)
Phloretin (300 μM)
100 mV
-80 mV
-100 mV
-80 mV
5 nA
500 ms

Fig. 8

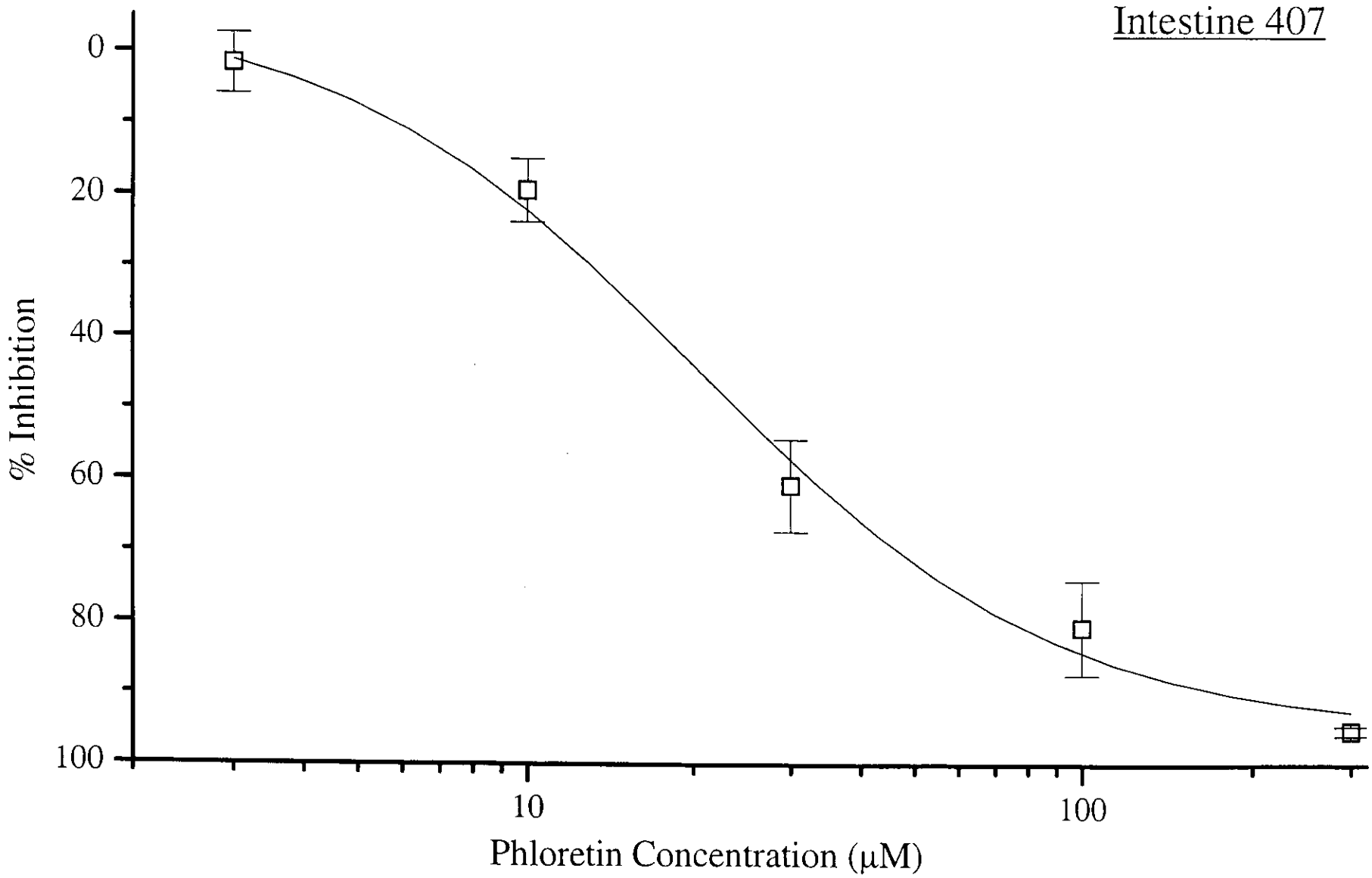
Intestine 407
0
20
40
60
80
100
% Inhibition
10
100
Phloretin Concentration (μM)

Fig. 9

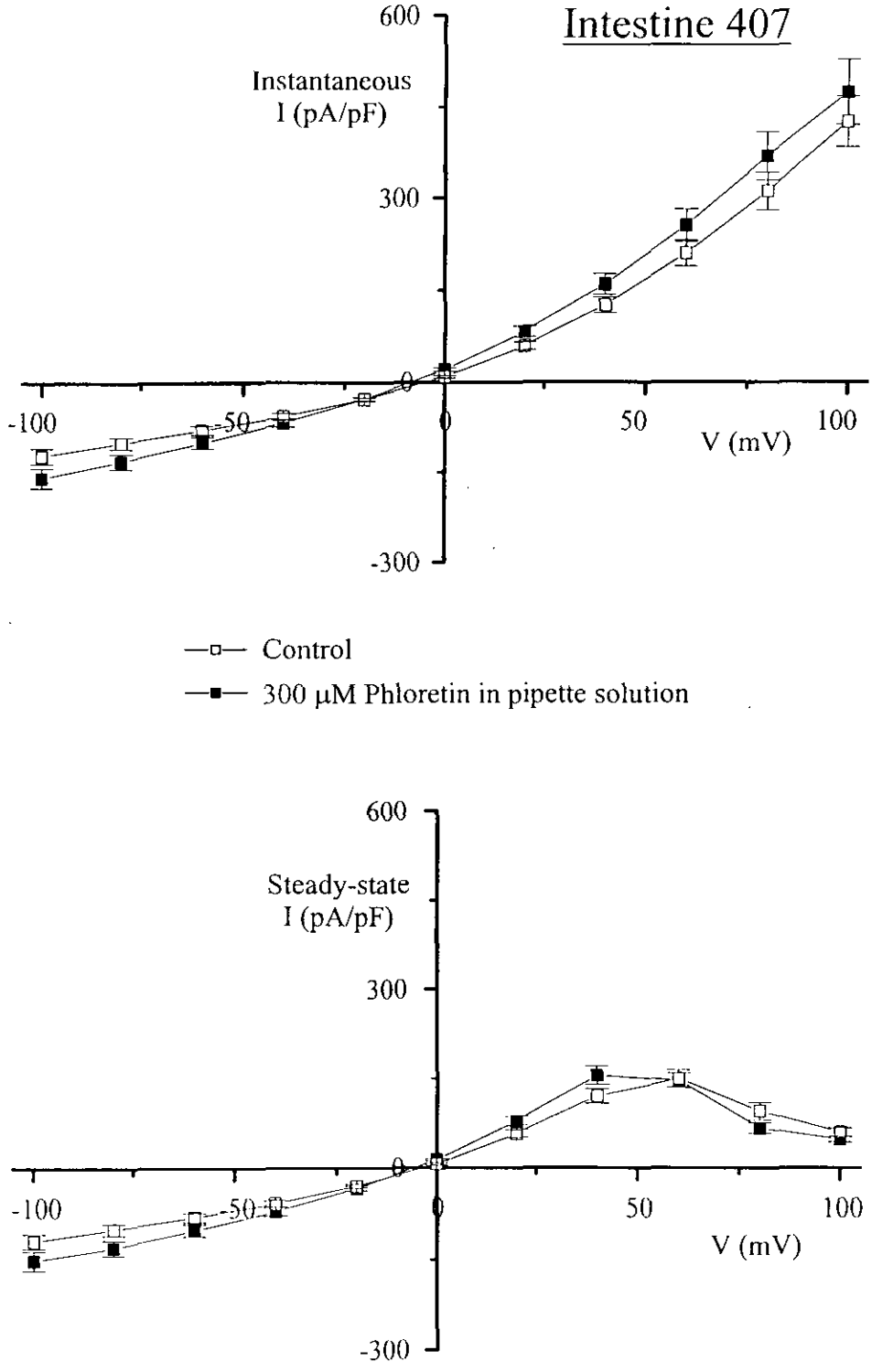
Intestine 407
Instantaneous
I (pA/pF)
600
300
-300
-100
-50
0
50
100
V (mV)
Control
300 μM Phloretin in pipette solution
Steady-state
I (pA/pF)
600
300
-300
-100
-50
0
50
100
V (mV)

Fig. 10

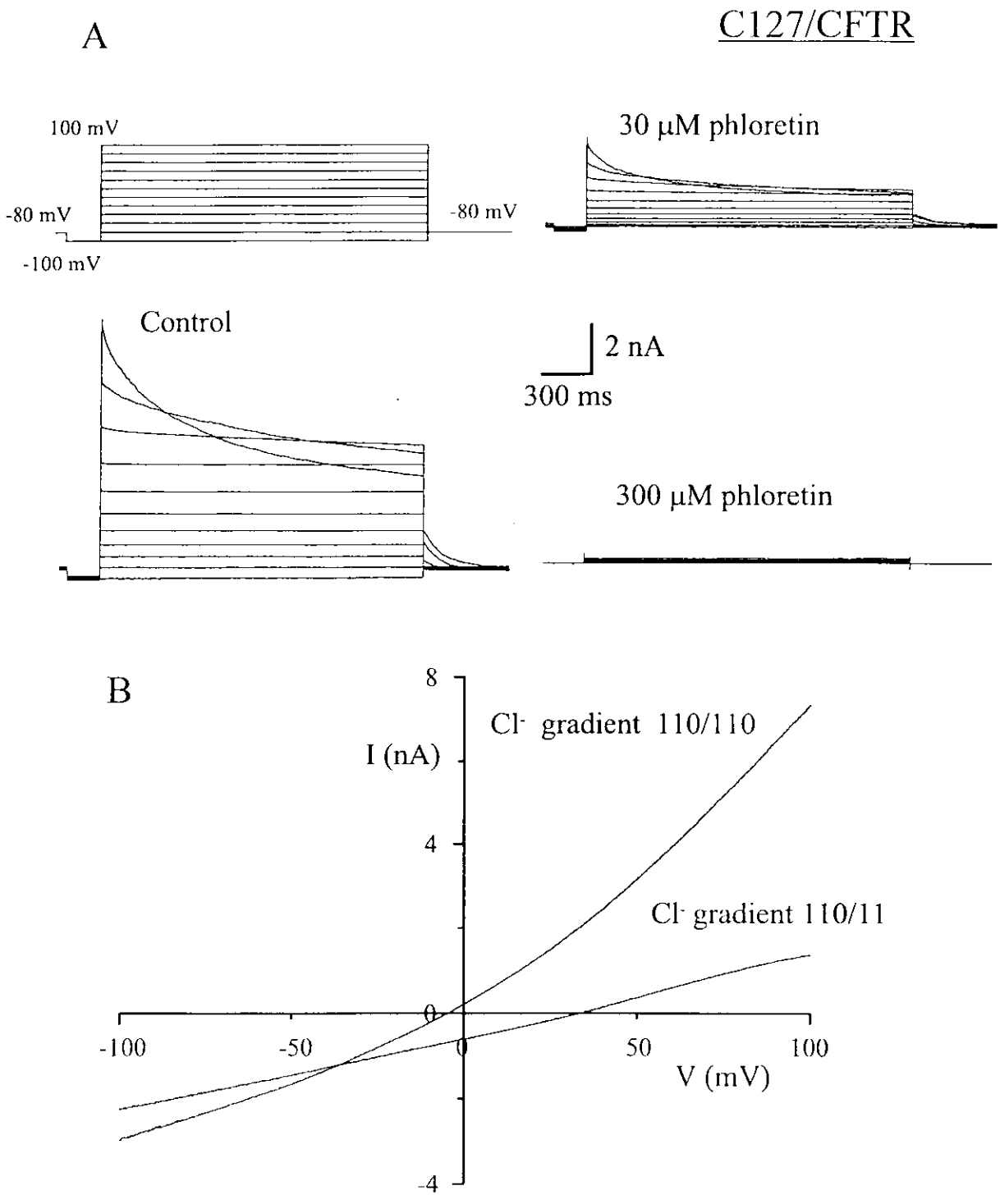
A
C127/CFTR
100 mV
-80 mV
-80 mV
-100 mV
30 μM phloretin
Control
2 nA
300 ms
300 μM phloretin
B
8
I (nA)
Cl- gradient 110/110
4
Cl- gradient 110/11
0
-100
-50
0
50
100
V (mV)
-4

Fig. 11

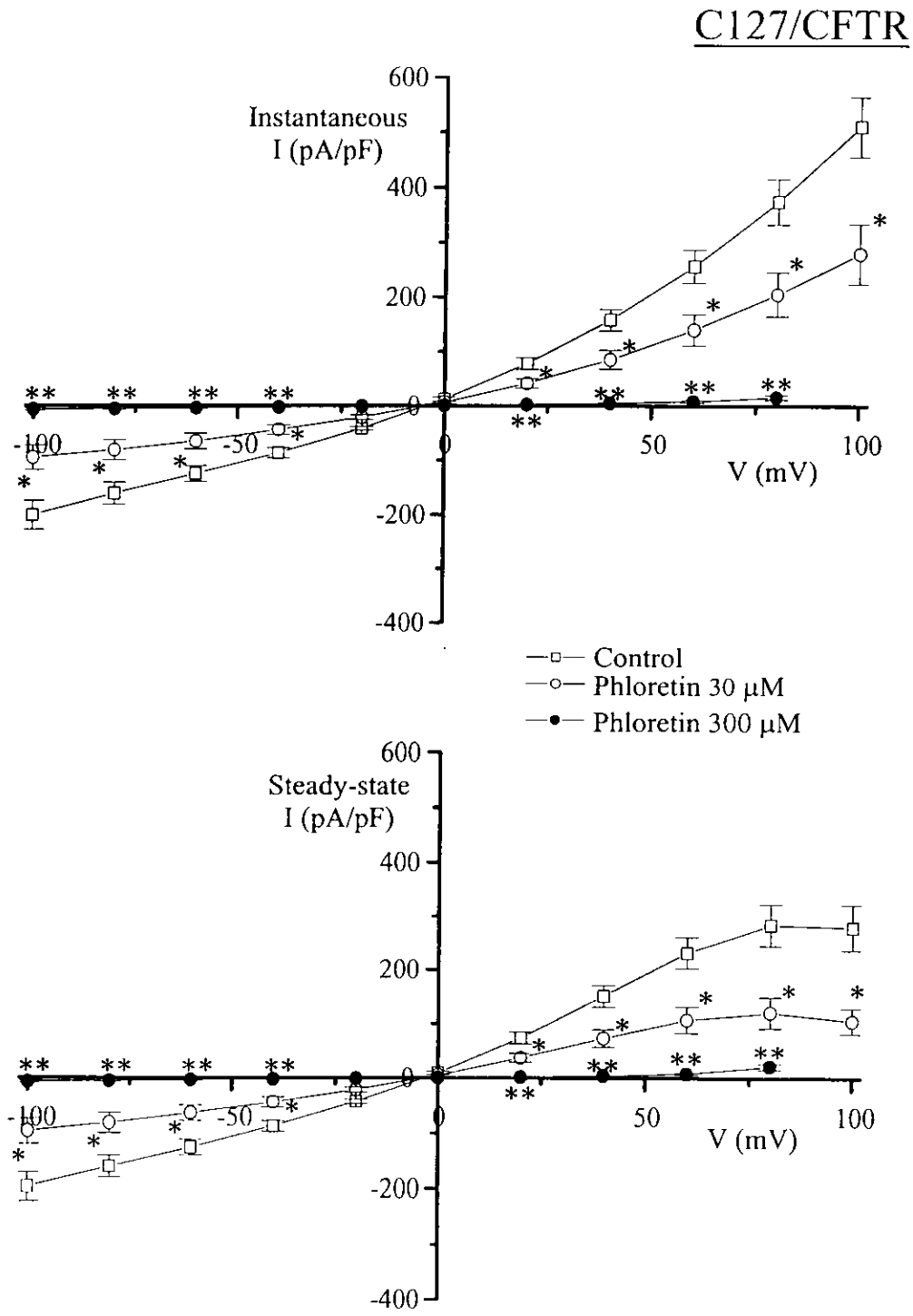
C127/CFTR
Instantaneous
I (pA/pF)
600
400
200
0
-200
-400
-100
-50
0
50
100
V (mV)
Control
Phloretin 30 μM
Phloretin 300 μM
Steady-state
I (pA/pF)
600
400
200
0
-200
-400
-100
-50
0
50
100
V (mV)

Fig. 12

Intestine 407

A

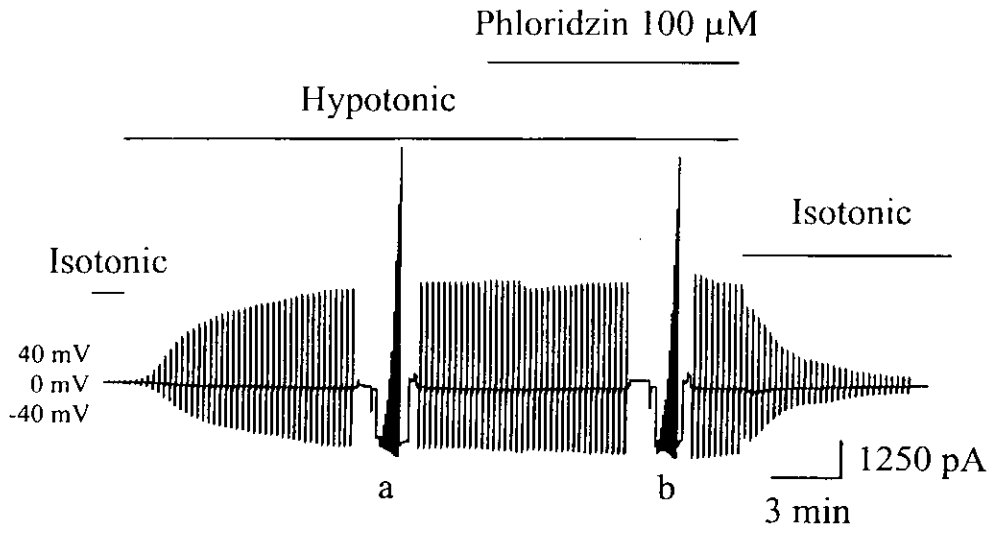

B

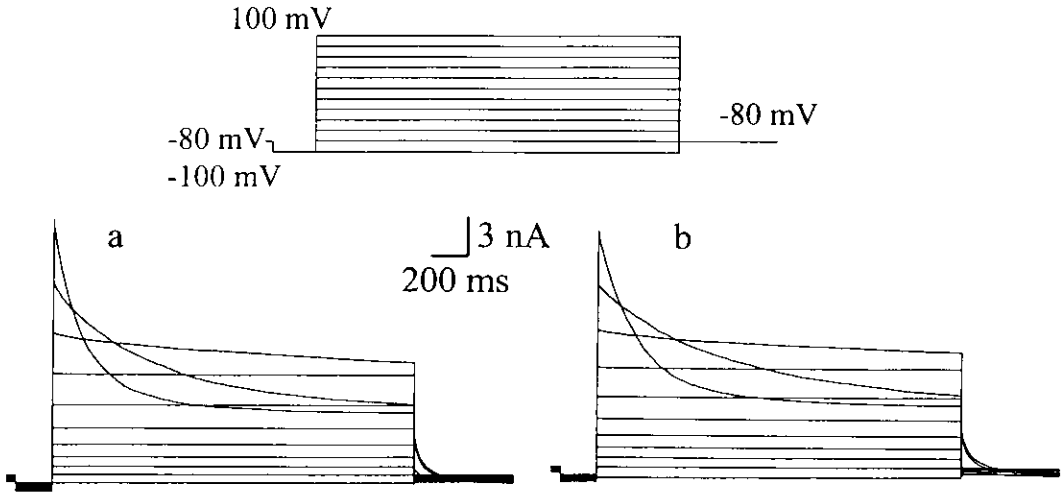

C

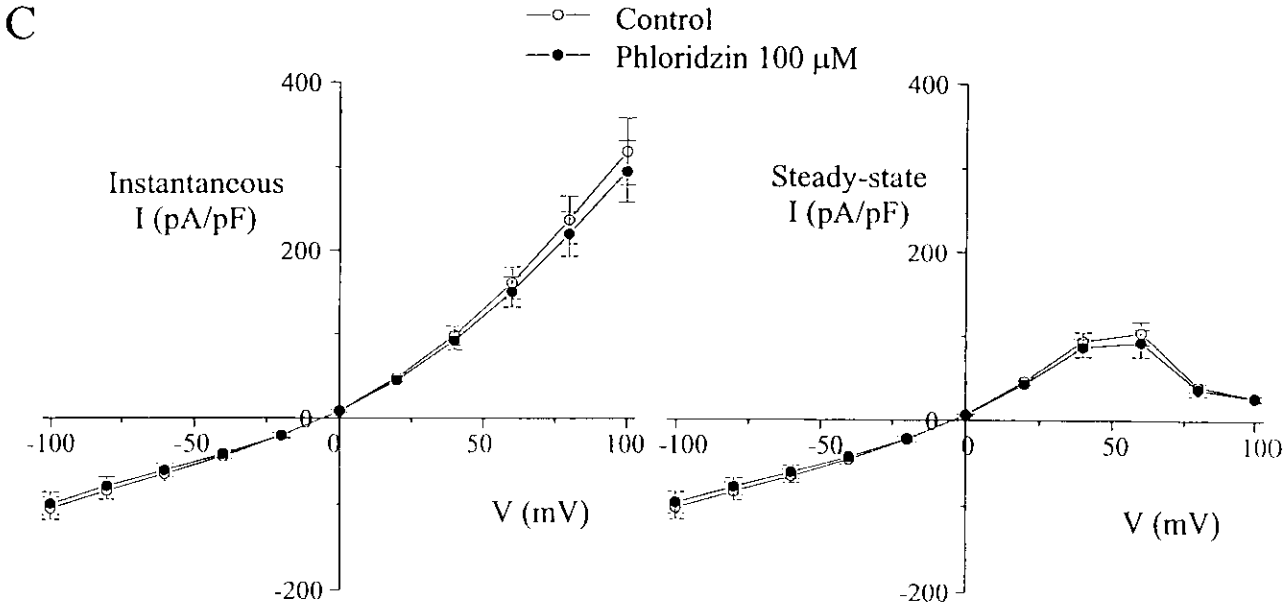

Fig. 13

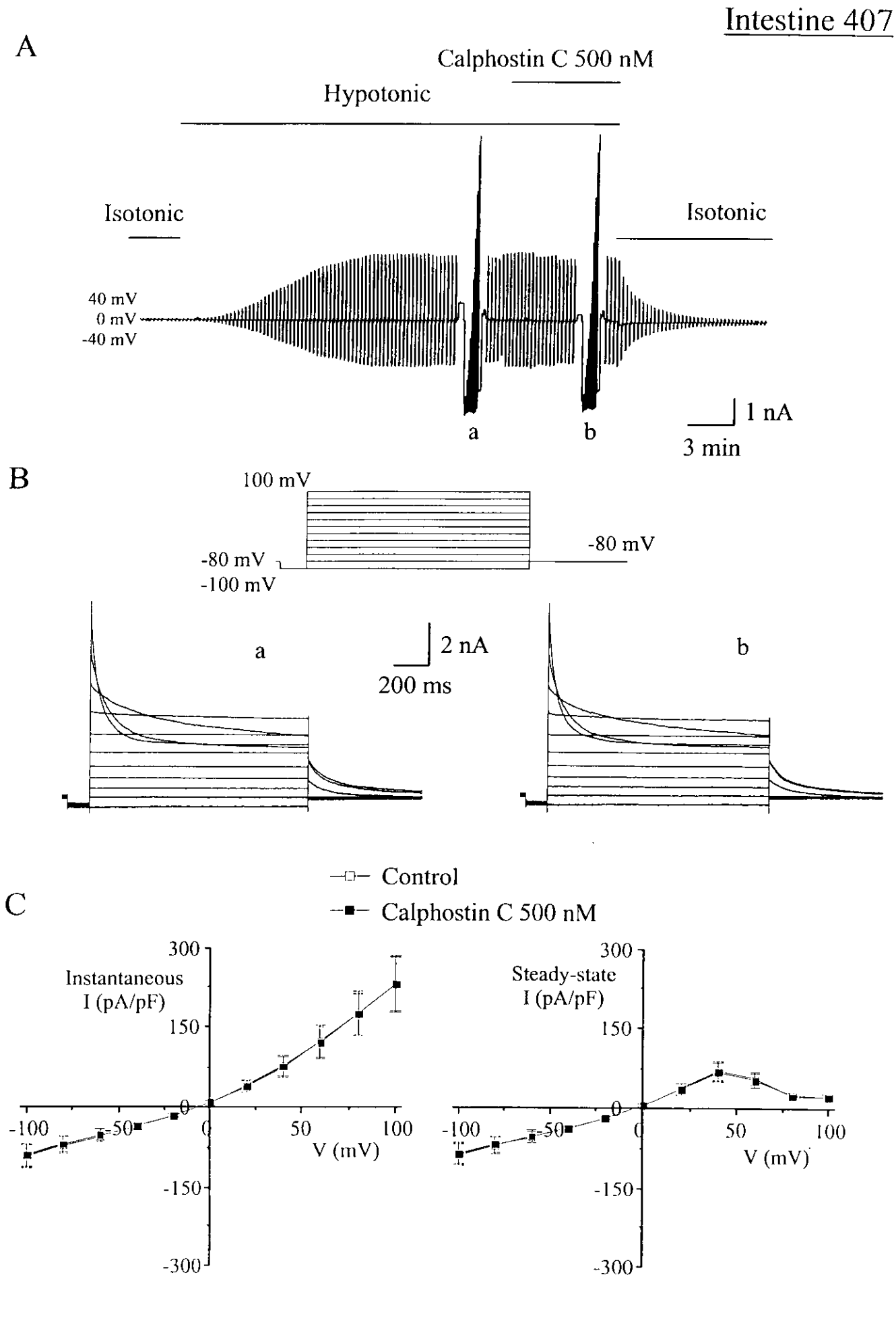
Intestine 407
A
Calphostin C 500 nM
Hypotonic
Isotonic
Isotonic
40 mV
0 mV
-40 mV
a
b
1 nA
3 min
B
100 mV
-80 mV
-100 mV
-80 mV
a
2 nA
200 ms
b
Control
Calphostin C 500 nM
C
Instantaneous
I (pA/pF)
Steady-state
I (pA/pF)
300
150
0
-150
-300
-100
-50
50
100
V (mV)

Fig. 14

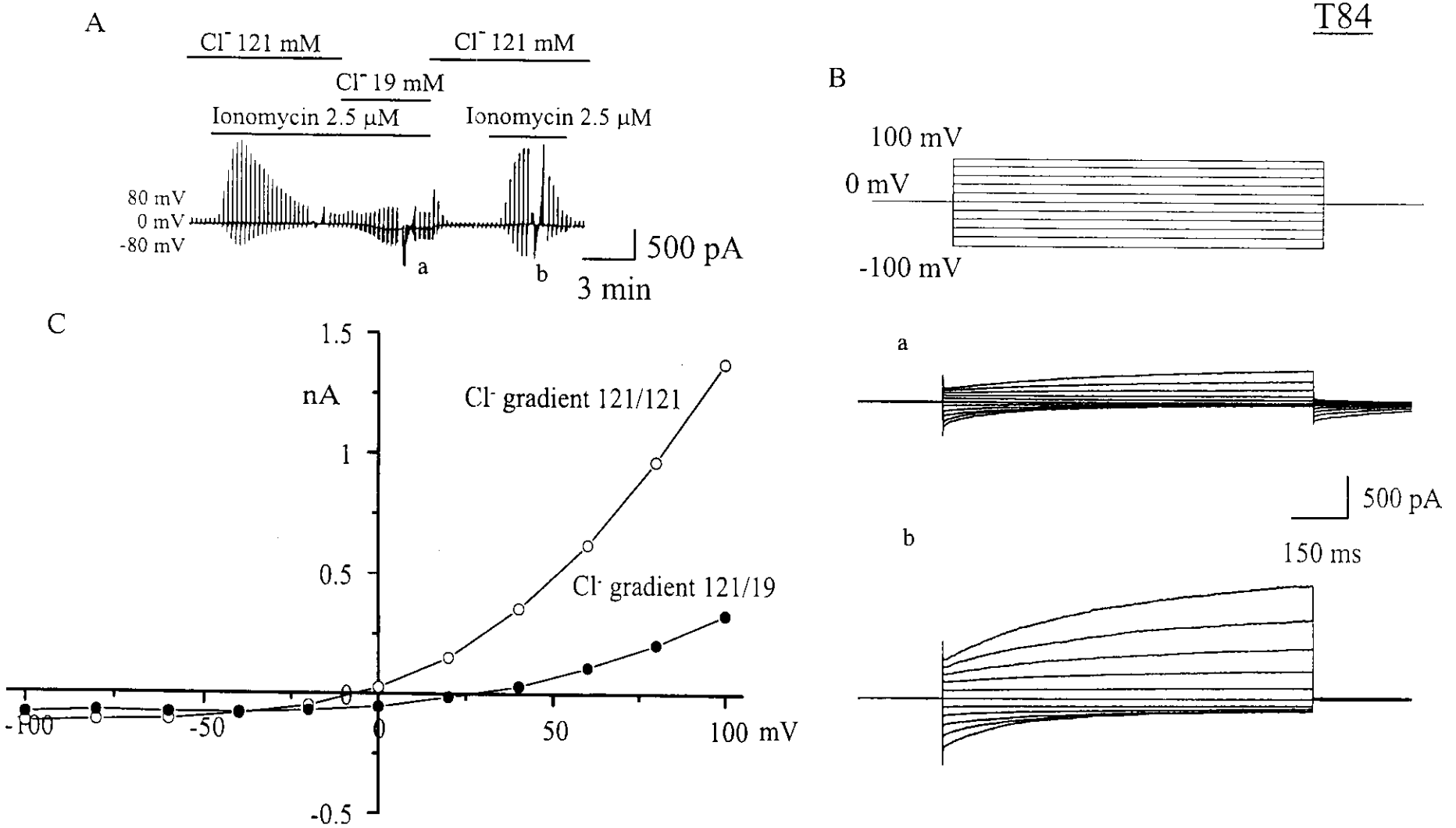
A
Cl⁻ 121 mM
Cl⁻ 121 mM
Cl⁻ 19 mM
Ionomycin 2.5 µM
Ionomycin 2.5 µM
80 mV
0 mV
-80 mV
a
b
500 pA
3 min
T84
B
100 mV
0 mV
-100 mV
a
500 pA
b
150 ms
C
1.5
nA
1
0.5
0
-0.5
Cl⁻ gradient 121/121
Cl⁻ gradient 121/19
-100
-50
0
50
100 mV

Fig. 15

A

T84

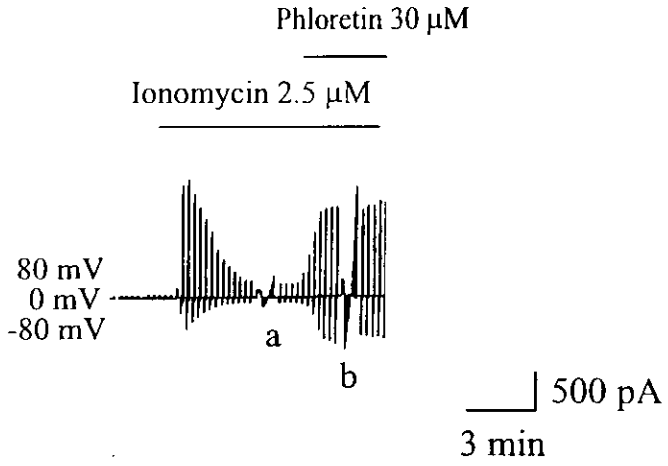

B

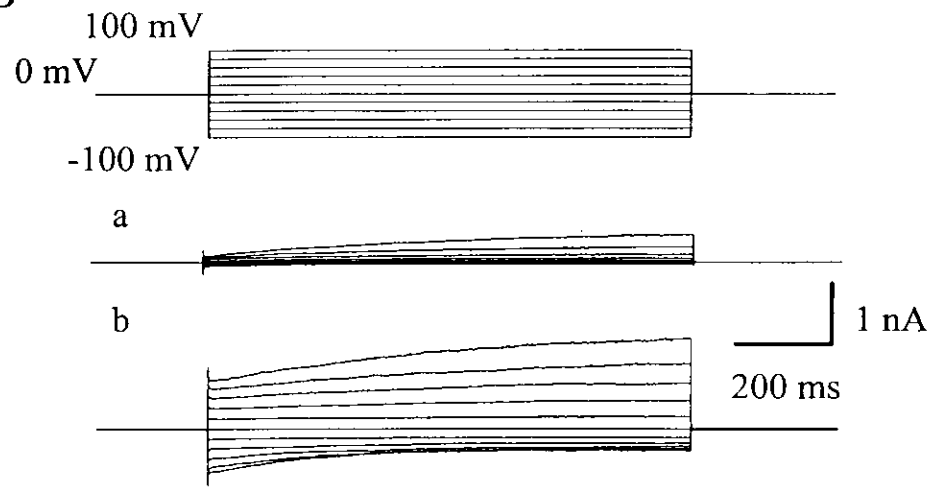

C

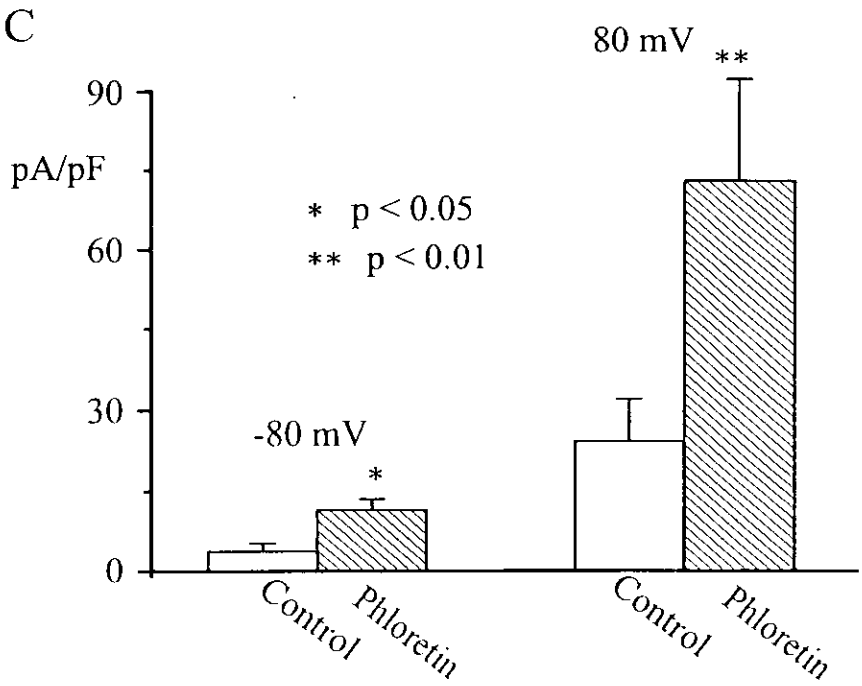

Fig. 16

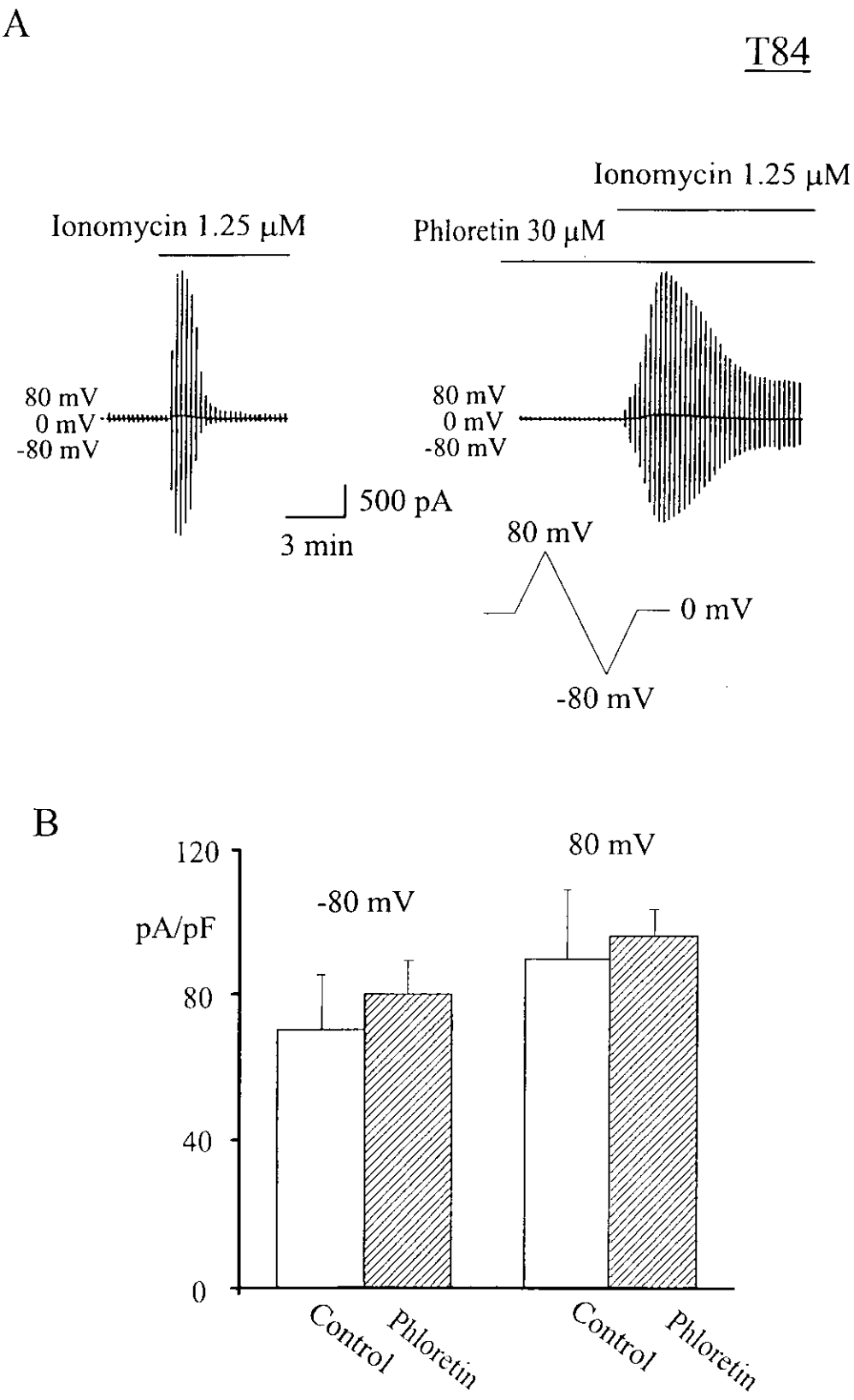
A
T84
Ionomycin 1.25 μM
Ionomycin 1.25 μM
Phloretin 30 μM
80 mV
0 mV
-80 mV
80 mV
0 mV
-80 mV
500 pA
3 min
80 mV
0 mV
-80 mV
B
120
pA/pF
80
40
0
-80 mV
80 mV
Control
Phloretin
Control
Phloretin

Fig. 17

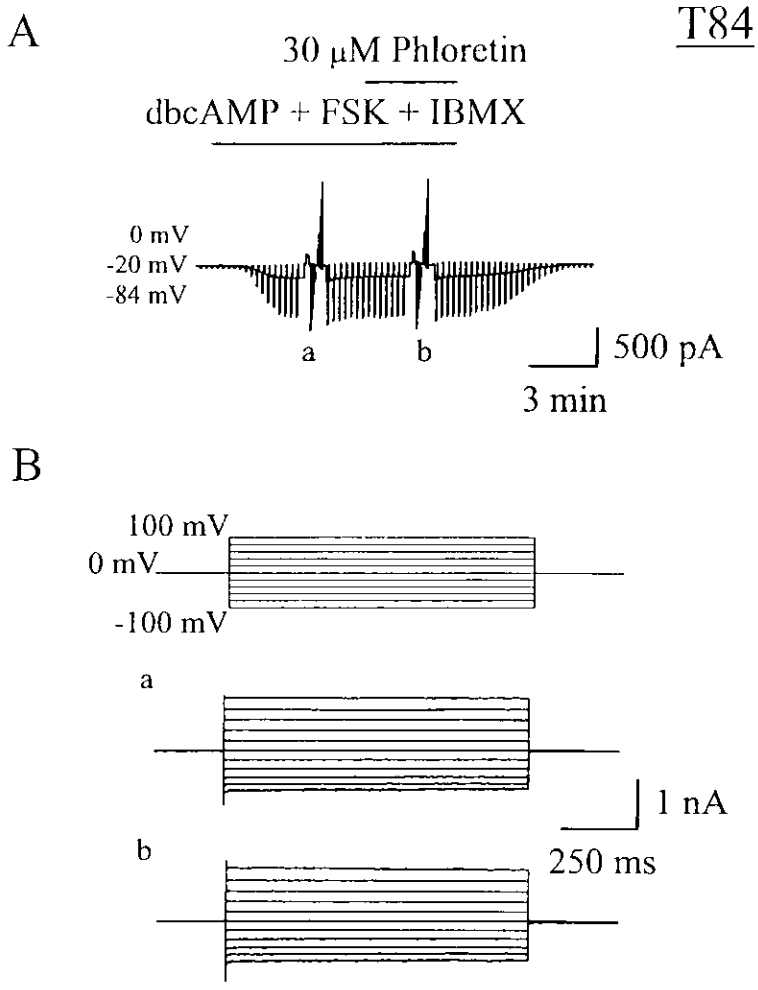
A
T84
30 μM Phloretin
dbcAMP + FSK + IBMX
0 mV
-20 mV
-84 mV
a
b
500 pA
3 min
B
100 mV
0 mV
-100 mV
a
1 nA
b
250 ms
C
Control
30 μM Phloretin
40
I (pA/pF)
20
0
-100
-50
0
50
100
V (mV)
-20
-40

Fig. 18

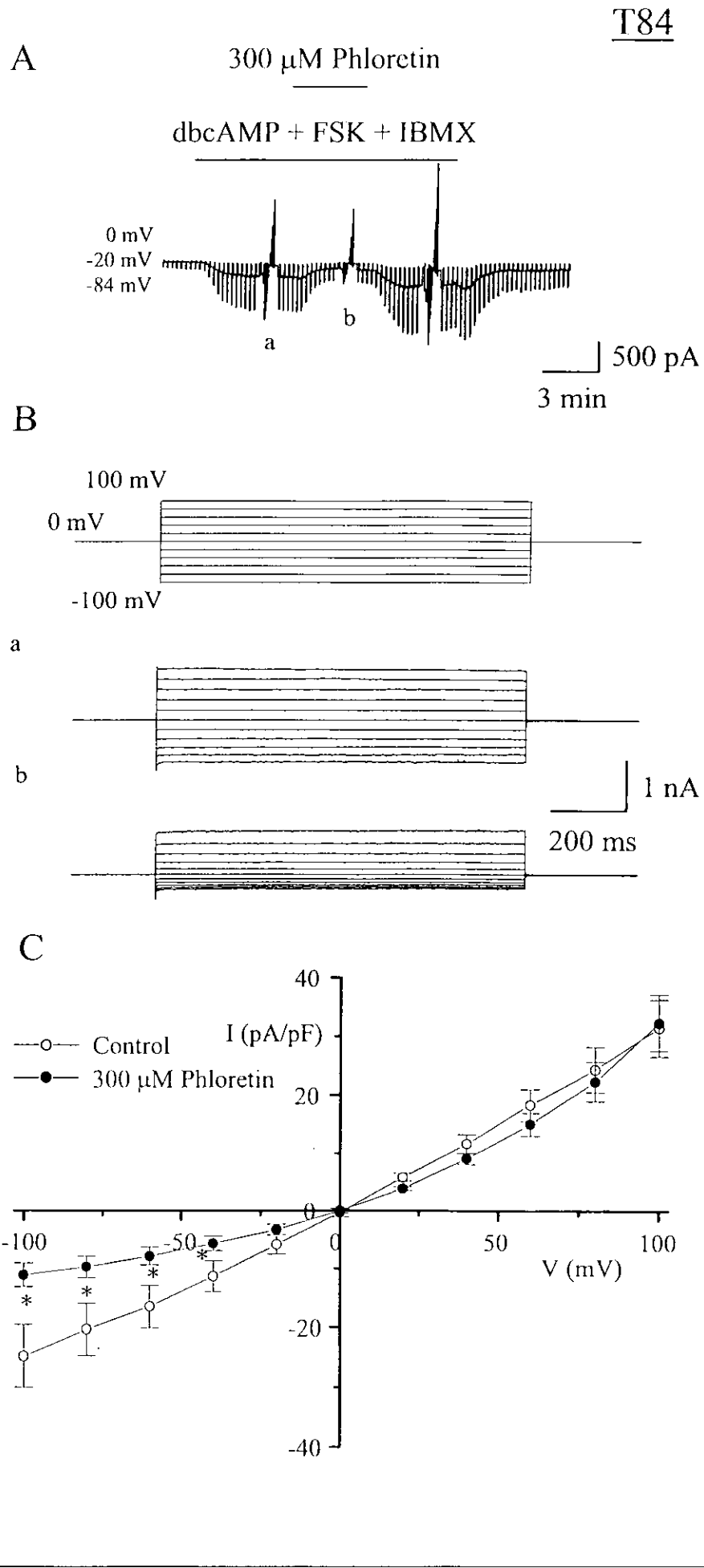
T84
A
300 μM Phloretin
dbcAMP + FSK + IBMX
0 mV
-20 mV
-84 mV
a
b
500 pA
3 min
B
100 mV
0 mV
-100 mV
a
b
1 nA
200 ms
C
40
20
0
-20
-40
I (pA/pF)
Control
300 μM Phloretin
-100
-50
0
50
100
V (mV)

Fig. 19

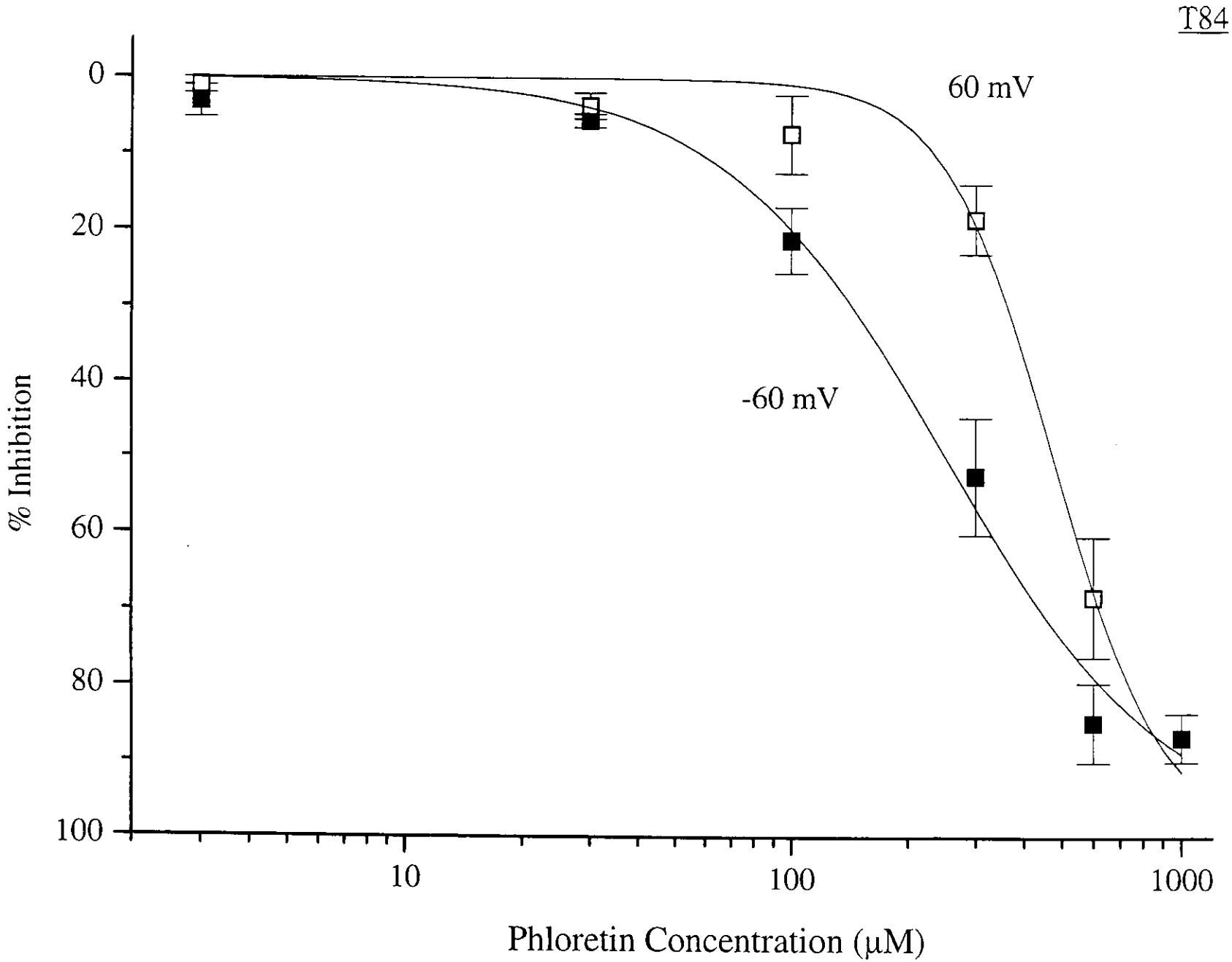
T84
60 mV
-60 mV
% Inhibition
0
20
40
60
80
100
10
100
1000
Phloretin Concentration (μM)

Fig. 20

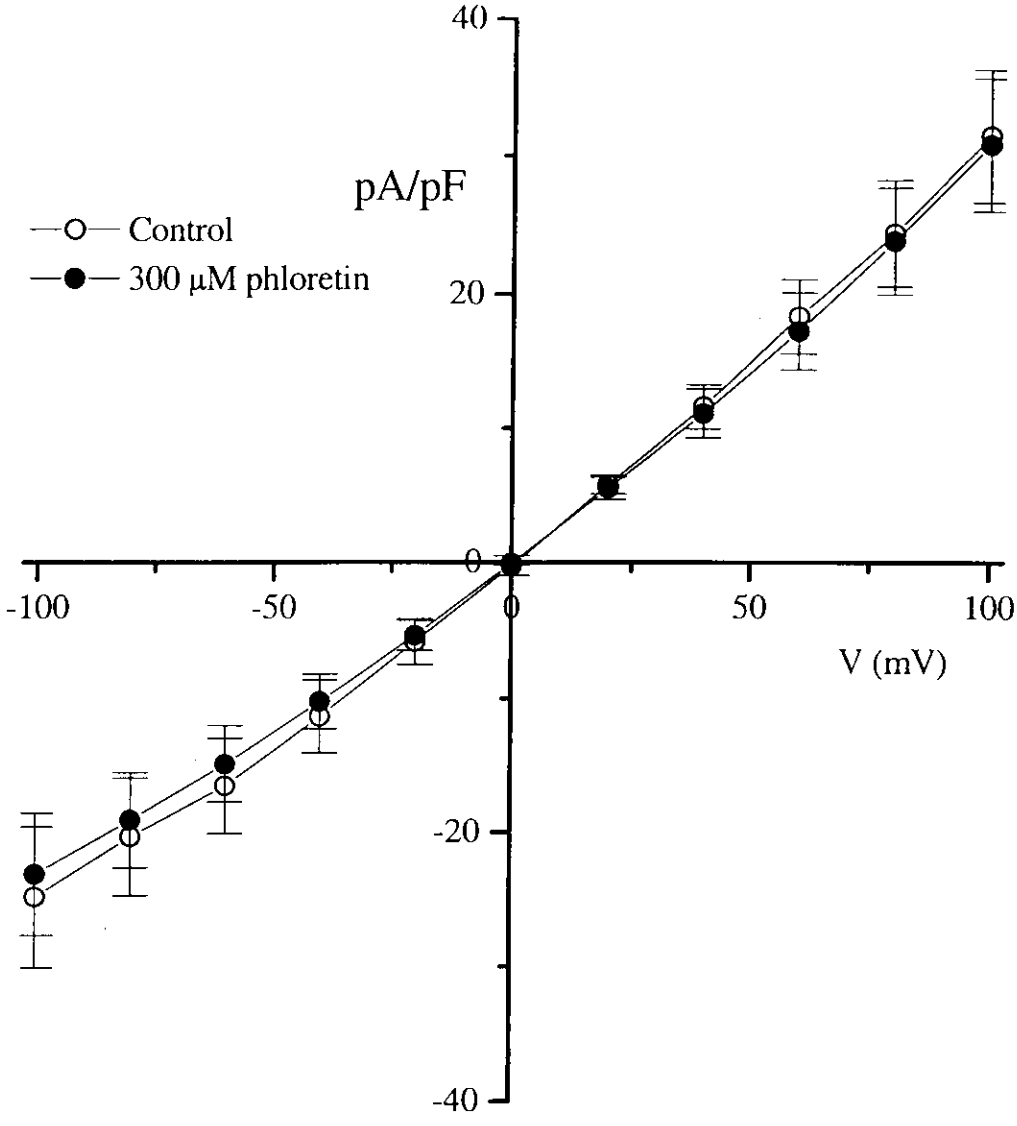

Fig. 21

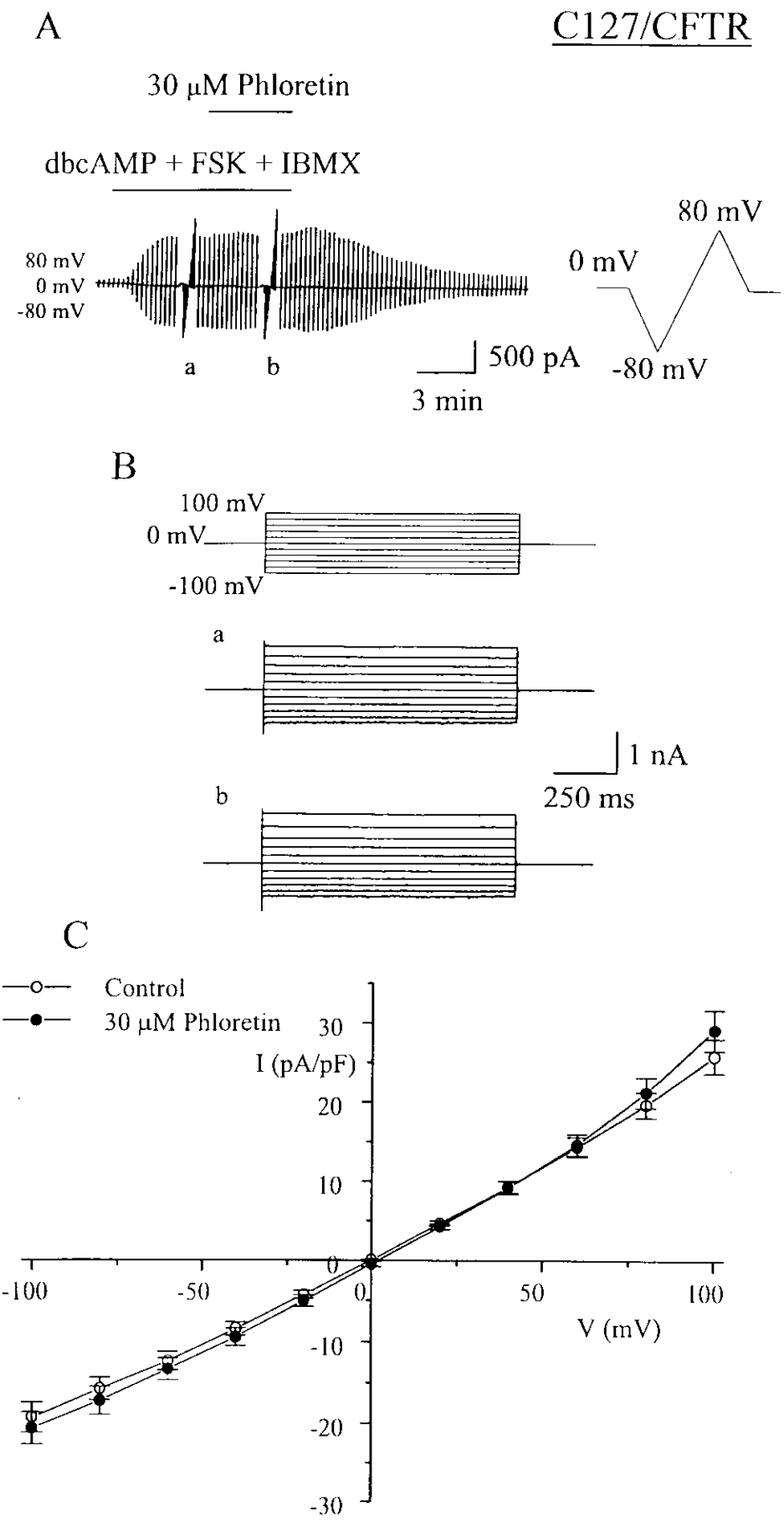
A
C127/CFTR
30 μM Phloretin
dbcAMP + FSK + IBMX
80 mV
0 mV
-80 mV
a
b
500 pA
3 min
80 mV
0 mV
-80 mV
B
100 mV
0 mV
-100 mV
a
b
1 nA
250 ms
C
Control
30 μM Phloretin
I (pA/pF)
V (mV)
30
20
10
0
-10
-20
-30
-100
-50
0
50
100

Fig. 22

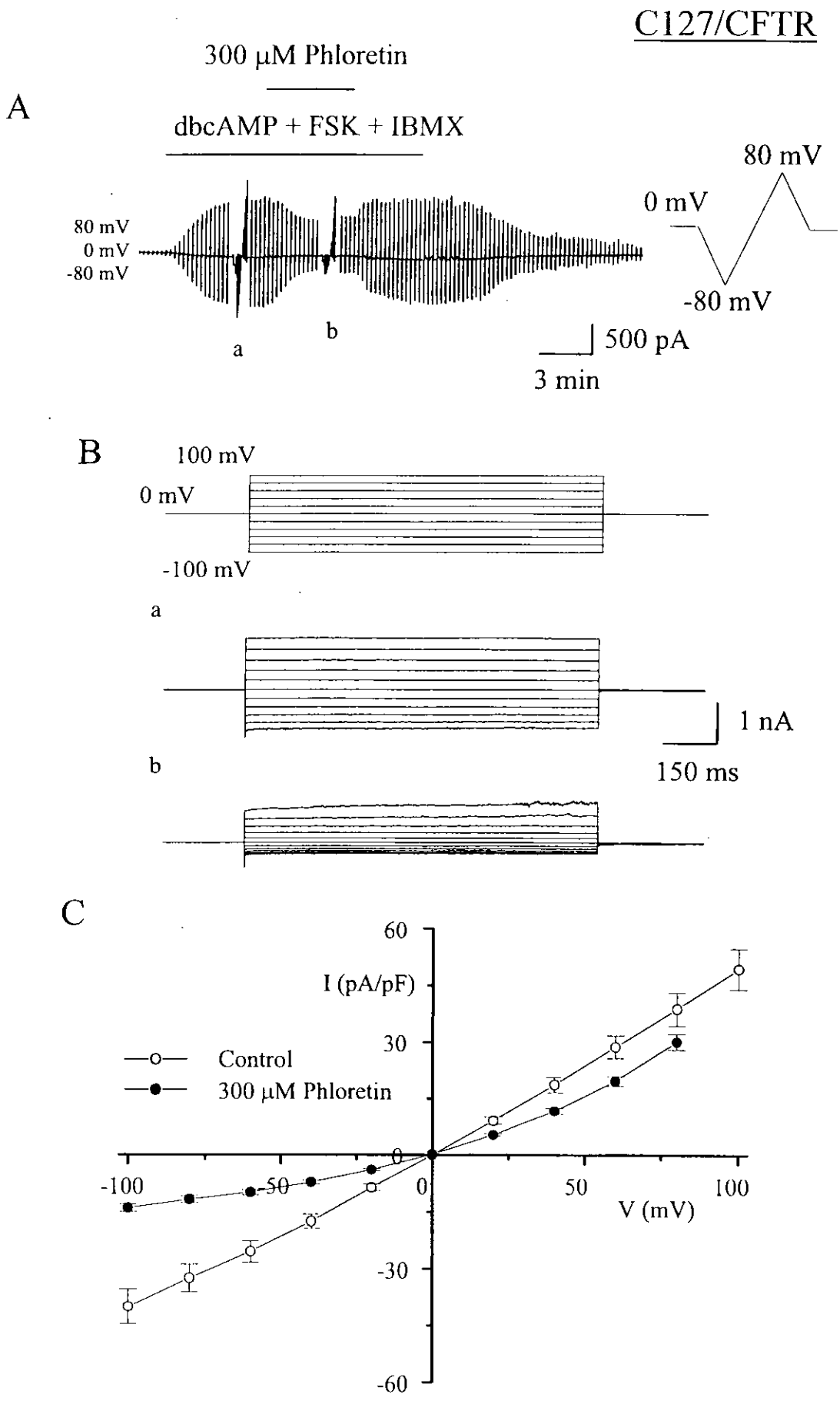
C127/CFTR
300 μM Phloretin
A
dbcAMP + FSK + IBMX
80 mV
0 mV
-80 mV
80 mV
0 mV
-80 mV
a
b
500 pA
3 min
B
100 mV
0 mV
-100 mV
a
1 nA
150 ms
b
C
60
I (pA/pF)
30
Control
300 μM Phloretin
0
-100
-50
0
50
100
V (mV)
-30
-60

Fig. 23

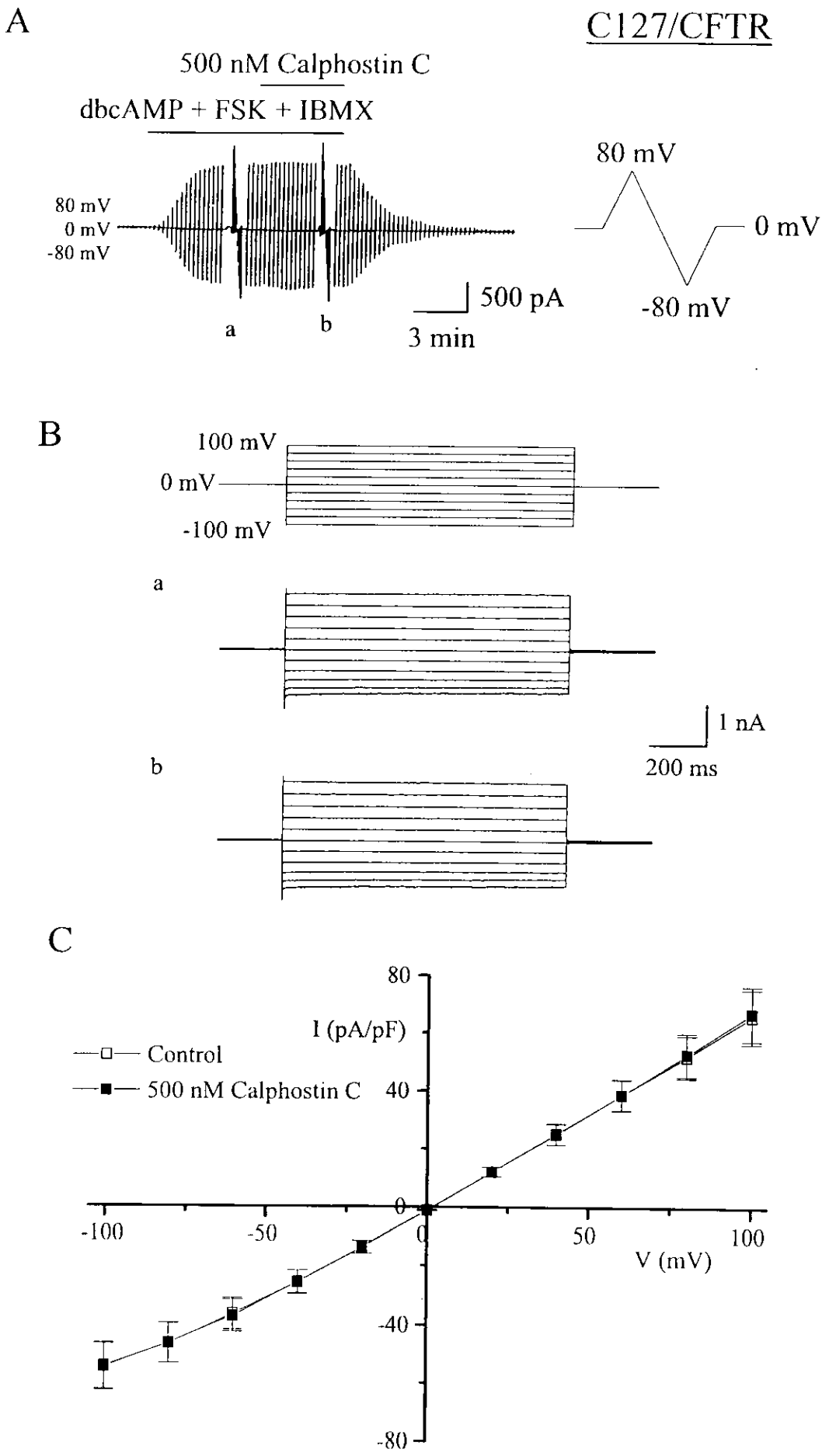
A
C127/CFTR
500 nM Calphostin C
dbcAMP + FSK + IBMX
80 mV
0 mV
-80 mV
500 pA
3 min
a
b
80 mV
0 mV
-80 mV
B
100 mV
0 mV
-100 mV
a
b
1 nA
200 ms
C
80
I (pA/pF)
Control
500 nM Calphostin C
40
0
-40
-80
-100
-50
0
50
100
V (mV)